A Micropeptide Encoded by a Putative Long Noncoding RNA Regulates Muscle Performance

ARTICLE *in* CELL · JANUARY 2015

Impact Factor: 32.24 · DOI: 10.1016/j.cell.2015.01.009 · Source: PubMed

Article

Cell

A Micropeptide Encoded by a Putative Long Noncoding RNA Regulates Muscle Performance

Graphical Abstract

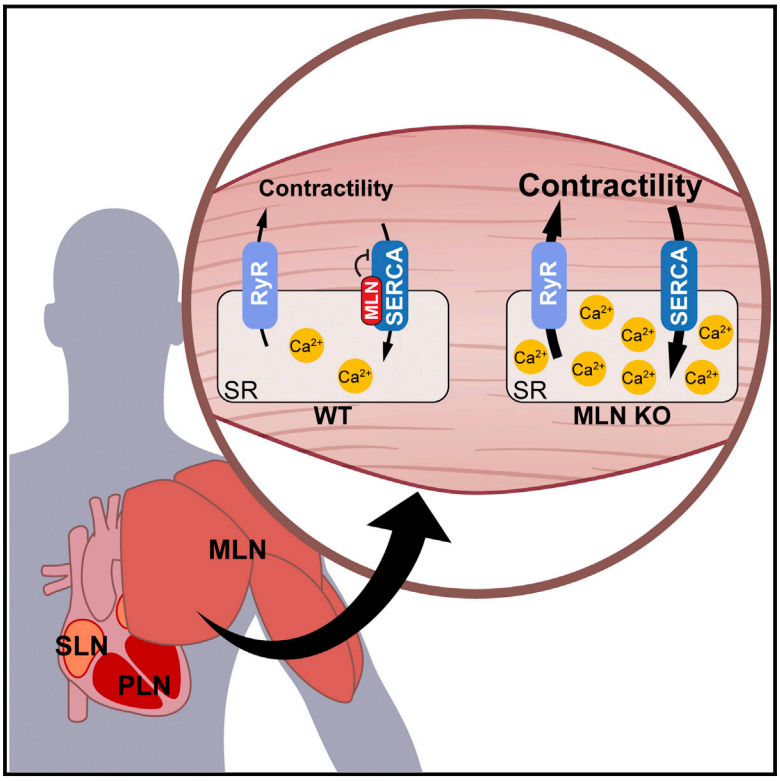

Authors

Douglas M. Anderson,
Kelly M. Anderson, ...,
Rhonda Bassel-Duby, Eric N. Olson

Correspondence

eric.olson@utsouthwestern.edu

In Brief

Myoregulin is a skeletal muscle-specific micropeptide that regulates muscle performance by modulating intracellular calcium handling.

Highlights

- Myoregulin is a micropeptide encoded by an annotated long noncoding RNA
- Myoregulin is a transmembrane alpha helix expressed only in skeletal muscle
- Myoregulin regulates Ca^{2+} handling by inhibiting the pump activity of SERCA
- Myoregulin KO mice show improved exercise performance and Ca^{2+} handling in muscle

Anderson et al., 2015, Cell *160*, 595–606
February 12, 2015
http://dx.doi.org/10.1016/j.cell.2015.01.009

CellPress

Cell

A Micropeptide Encoded by a Putative Long Noncoding RNA Regulates Muscle Performance

Douglas M. Anderson,[1,4] Kelly M. Anderson,[1,4] Chi-Lun Chang,[2] Catherine A. Makarewich,[1,4] Benjamin R. Nelson,[1,4] John R. McAnally,[1,4] Prasad Kasaragod,[1] John M. Shelton,[3] Jen Liou,[2] Rhonda Bassel-Duby,[1,4] and Eric N. Olson[1,4,*]
[1]Department of Molecular Biology
[2]Department of Physiology
[3]Department of Internal Medicine
[4]Hamon Center for Regenerative Science and Medicine
The University of Texas Southwestern Medical Center, 5323 Harry Hines Boulevard, Dallas, TX 75390–9148, USA
*Correspondence: eric.olson@utsouthwestern.edu
http://dx.doi.org/10.1016/j.cell.2015.01.009

SUMMARY

Functional micropeptides can be concealed within RNAs that appear to be noncoding. We discovered a conserved micropeptide, which we named myoregulin (MLN), encoded by a skeletal muscle-specific RNA annotated as a putative long noncoding RNA. MLN shares structural and functional similarity with phospholamban (PLN) and sarcolipin (SLN), which inhibit SERCA, the membrane pump that controls muscle relaxation by regulating Ca^{2+} uptake into the sarcoplasmic reticulum (SR). MLN interacts directly with SERCA and impedes Ca^{2+} uptake into the SR. In contrast to PLN and SLN, which are expressed in cardiac and slow skeletal muscle in mice, MLN is robustly expressed in all skeletal muscle. Genetic deletion of MLN in mice enhances Ca^{2+} handling in skeletal muscle and improves exercise performance. These findings identify MLN as an important regulator of skeletal muscle physiology and highlight the possibility that additional micropeptides are encoded in the many RNAs currently annotated as noncoding.

INTRODUCTION

Ca^{2+} controls the normal function of striated muscle by acting as the primary regulator of the sarcomeric contractile machinery and as a second messenger in the signal transduction pathways that control muscle growth, metabolism, and pathological remodeling (Bassel-Duby and Olson, 2006; Berchtold et al., 2000). Ca^{2+} handling in striated muscle is tightly regulated by Ca^{2+} pumps in the sarcoplasmic reticulum (SR) and plasma membranes that maintain intracellular Ca^{2+} levels ~10,000-fold lower than extracellular and SR concentrations (Berridge et al., 2003; Rossi and Dirksen, 2006). Upon muscle stimulation, Ca^{2+} release by the ryanodine receptor (RyR) in the SR membrane transiently increases Ca^{2+} levels in the cytosol, triggering actomyosin cross-bridge formation within the sarcomere to generate contractile force. Reuptake of Ca^{2+} into the SR by sarcoplasmic reticulum Ca^{2+}-ATPase (SERCA) is necessary for muscle relaxation and restores SR Ca^{2+} levels for subsequent contraction-relaxation cycles. SERCA serves as a central regulator of striated muscle performance and the pathological signaling pathways that drive cardiovascular and skeletal muscle disease (Dorn and Molkentin, 2004; Goonasekera et al., 2011; Odermatt et al., 1996; Pan et al., 2003; Periasamy and Kalyanasundaram, 2007).

Two related peptides, phospholamban (PLN) and sarcolipin (SLN), directly interact with SERCA in the SR membrane to regulate Ca^{2+} pump activity (Kranias and Hajjar, 2012; MacLennan and Kranias, 2003). PLN and SLN are expressed in partially overlapping patterns in cardiac and slow skeletal muscle and are important regulators of muscle performance and cardiovascular disease (Briggs et al., 1992; Kranias and Hajjar, 2012; Minamisawa et al., 2003; Schmitt et al., 2003; Tada and Toyofuku, 1998; Tupling et al., 2011). PLN-deficient mice exhibit enhanced myocardial contractile performance, characterized by increased ventricular relaxation rates and SERCA pump activity (Chu et al., 1998; Luo et al., 1994). Similarly, loss of PLN or SLN expression significantly increases the rate of muscle relaxation and SERCA pump activity in slow skeletal muscle but does not affect fast skeletal muscles, which do not express PLN or SLN (Slack et al., 1997; Tupling et al., 2011; Vangheluwe et al., 2005). The absence of PLN and SLN expression in fast skeletal muscle, the dominant muscle type in mice, suggests that an unidentified factor regulates Ca^{2+} handling and the contractile performance of this tissue.

Recent genome-wide studies have suggested that hundreds of functional micropeptides may be encoded in vertebrate long noncoding RNAs (lncRNAs) (Andrews and Rothnagel, 2014; Bazzini et al., 2014). The microproteome has largely been overlooked in gene annotations, primarily because of the difficulty in identifying functional small open reading frames (ORFs) in RNA transcripts. While analyzing an annotated skeletal muscle-specific lncRNA, we discovered a previously unrecognized ORF encoding a conserved 46 amino acid micropeptide, which we named myoregulin (MLN). MLN forms a single transmembrane alpha helix that interacts with SERCA in the membrane of the SR and regulates Ca^{2+} handling. Consistent with this function, deletion of MLN in mice significantly enhances Ca^{2+} handling and improves exercise performance. These findings identify MLN as the predominant SERCA-inhibitory

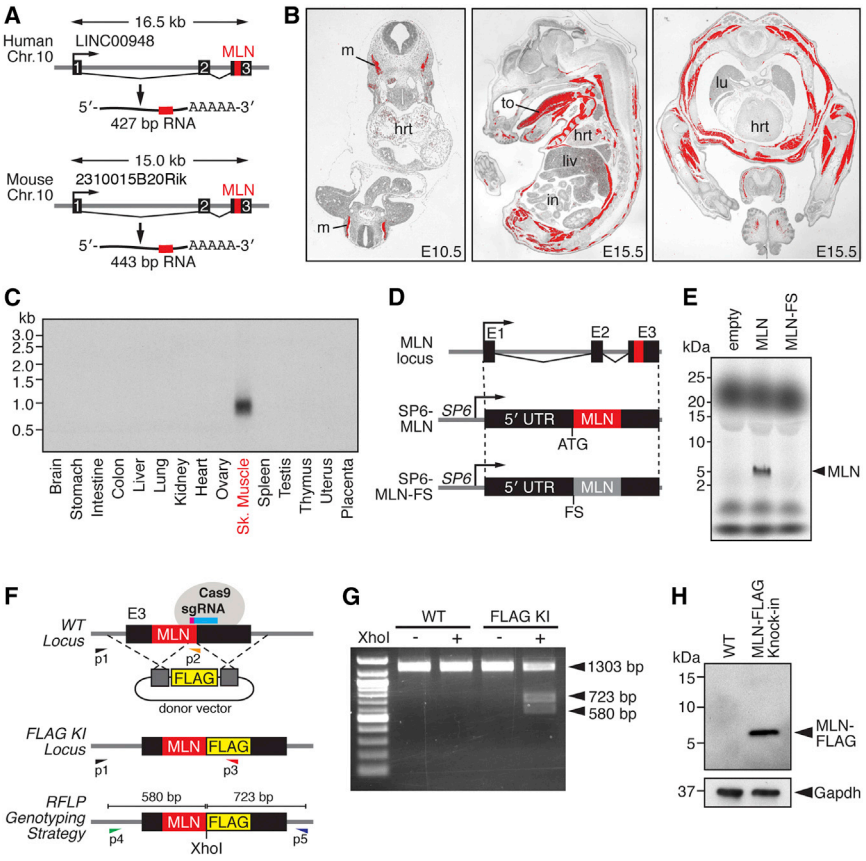

Figure 1. Discovery of a Skeletal Muscle-Specific Micropeptide

(A) A short ORF encoding a conserved micropeptide, which we named myoregulin (MLN), is contained within exon 3 of an annotated lncRNA in human and mouse genomes. The position of the MLN ORF is indicated in red.

(B) In situ hybridization showing skeletal muscle-specific expression of MLN at the indicated embryonic time points. hrt, heart; in, intestine; liv, liver; lu, lung; m, myotome; to, tongue.

(C) Northern blot of RNA isolated from adult mouse tissues using a probe specific to the full-length MLN transcript shows skeletal muscle-specific expression.

(D) Diagram of the constructs used for in vitro translation of the MLN micropeptide. The full-length MLN RNA transcript was subcloned into the CS2 vector containing the SP6 phage RNA polymerase promoter (SP6-MLN). A frameshift mutation was introduced immediately after the endogenous ATG to disrupt the MLN ORF (SP6-MLN-FS).

(E) Coupled in vitro transcription and translation reactions of the SP6-MLN vector using radiolabeled ^{35}S-methionine produced a ~5 kDa micropeptide, visualized by Tricine SDS-PAGE. The frameshift mutation in the MLN ORF (SP6-MLN-FS) abolished any detectable expression.

(F) Targeting strategy using CRISPR/Cas9-mediated homologous recombination to knock in a FLAG epitope tag into the MLN locus in C2C12 cells. PCR-based genotyping using primers (P1–P3) or RFLP analysis of PCR products generated using primers (P4 and P5) was used to verify correct targeting.

(G) RFLP analysis of WT C2C12 and heterozygous C2C12 myoblasts for the MLN-FLAG knockin allele.

(H) Western blot analysis showing endogenous expression of the MLN-FLAG fusion peptide in differentiated C2C12 myotubes, detected with an anti-FLAG antibody.

See also Figure S1.

micropeptide in skeletal muscle, which surprisingly was concealed in an RNA annotated as noncoding.

RESULTS

Discovery of a Conserved Micropeptide Encoded by a lncRNA

In a bioinformatic screen for uncharacterized skeletal muscle-specific genes, we identified a vertebrate RNA transcript annotated as a lncRNA (LINC00948 in humans and 2310015B20Rik in mice). Analysis of the evolutionary conservation of these transcripts identified a short 138 nucleotide ORF with the potential to encode a highly conserved 46 amino acid micropeptide, which we named myoregulin (MLN) (Figure S1A available online). The human and mouse MLN genes consist of three exons that span 16.5 and 15.0 kb, respectively, with the ORF located in exon 3 (Figure 1A). Nucleotide insertions and deletions that could alter the reading frame flank the MLN ORF, demonstrating that these sequences comprise UTRs (Figure S1A).

During embryogenesis, MLN is expressed in the myotomal compartment of the somites, the anlagen of skeletal muscle (Figure 1B). During fetal and adult stages, MLN is robustly expressed in all skeletal muscles and is not detectable in cardiac or smooth muscles (Figures 1B and 1C). MLN transcripts are also present in C2C12 myoblasts and myotubes, but not in 10T1/2 fibroblasts (Figure S1B).

To determine if the MLN ORF is translated as a micropeptide, we transcribed and translated the full-length MLN RNA in vitro in the presence of radiolabeled ^{35}S-methionine (Figures 1D and 1E). A single ~5 kDa micropeptide was produced from the MLN transcript, whereas a frameshift mutation that disrupted the MLN ORF abolished any detectable expression (Figures 1D and 1E). We further cloned a FLAG epitope tag in-frame with the C terminus of the MLN coding sequence within the full-length MLN transcript (Figure S1C). Expression of this construct in COS7 cells yielded a peptide of ~6 kDa, corresponding to the predicted molecular weight of the MLN-FLAG fusion peptide, detected by western blot (Figure S1D).

To determine whether MLN is endogenously expressed in skeletal muscle, we introduced the same FLAG epitope tag into the MLN locus in C2C12 muscle cells using CRISPR/Cas9-mediated homologous recombination (Figures 1F and S1E). PCR-based genotyping and restriction fragment-length polymorphism (RFLP) analyses were used to verify correct targeting (Figures 1G and S1F). As shown by western blot analysis in Figure 1H, C2C12 cells heterozygous for the MLN-FLAG

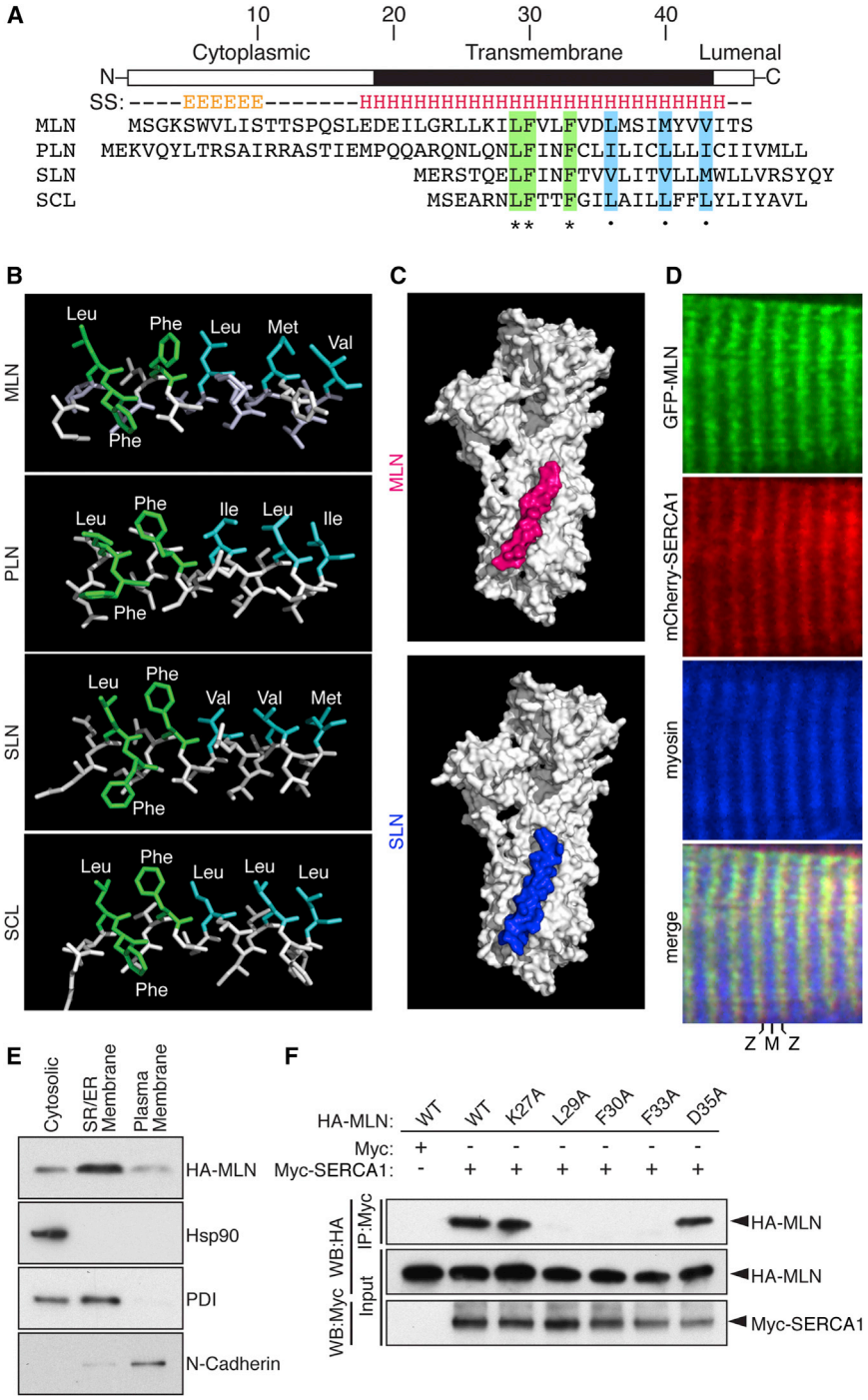

Figure 2. MLN Forms a Transmembrane Alpha Helix that Interacts with SERCA

(A) The secondary structure (SS) of MLN is predicted to contain an N-terminal beta sheet and C-terminal transmembrane alpha helix (E, beta sheet; H, alpha helix). Alignment of mouse MLN, PLN, SLN, and the invertebrate ortholog SCL identified identical (green) and similar (blue) residues conserved in all four micropeptides.

(B) The structure of the transmembrane helices of MLN, SLN, PLN, and SCL was modeled using I-TASSER and showed a common spatial orientation of conserved residues.

(C) Automated protein docking using ClusPro predicted that MLN occupies the same groove in SERCA1 that is recognized by SLN.

(D) Two-photon laser scanning confocal microscopy showing colocalization of GFP-MLN and mCherry-SERCA1 fusion proteins in the SR of mature skeletal muscle fibers. M, M-line; Z, Z-line.

(E) Retroviral expression of an N-terminal HA-tagged MLN fusion peptide (HA-MLN) in C2C12 myoblasts was enriched in the subcellular fraction containing SR/ER membrane proteins. Enrichment for cytosolic, SR/ER membrane, and plasma membrane proteins was verified by western blot analysis for Hsp90, PDI, and N-cadherin, respectively.

(F) Coimmunoprecipitation (coIP) experiments with HA-tagged MLN alanine mutants and a Myc-tagged SERCA1 construct transfected into COS7 cells identified residues important for interaction of MLN with SERCA1. Interaction of MLN with SERCA1 was abolished by mutation of residues shared with PLN, SLN, and SCL (L29A, F30A, and F33A), but not by the charged residues K27A or D35A. Western blot performed with anti-HA (WB-HA) or anti-Myc (WB-Myc).

See also Figure S2.

knockin allele expressed a micropeptide of the predicted molecular weight of the MLN-FLAG fusion peptide. Together, these data reveal that the MLN RNA, which is annotated as noncoding, in fact encodes a cryptic micropeptide.

MLN Encodes a Transmembrane Alpha Helix

The MLN micropeptide is highly conserved across mammals and is predicted to form a type II single-pass transmembrane alpha helix in which the 19 N-terminal amino acid residues are exposed to the cytosol and the three C-terminal residues are lumenal (Figures 2A and S2A). The N-terminal residues (5–10) of MLN are predicted to fold into a small beta sheet, and the C-terminal half of the protein contains the predicted transmembrane alpha helix (Figures 2A and S2A). Circular dichroism spectroscopy measurements of synthesized full-length MLN peptide in detergent micelles confirmed it consists of alpha helix (43.6%), beta sheet (21.1%), turn (9.6%), and random coil (25.7%) structures (Figure S2B).

Association of MLN with SERCA

MLN shows a strong structural resemblance to PLN and SLN, which also form type II single-pass transmembrane peptides oriented with their N-terminal residues exposed to the cytosol. Sequence alignment of MLN, PLN, and SLN revealed a number

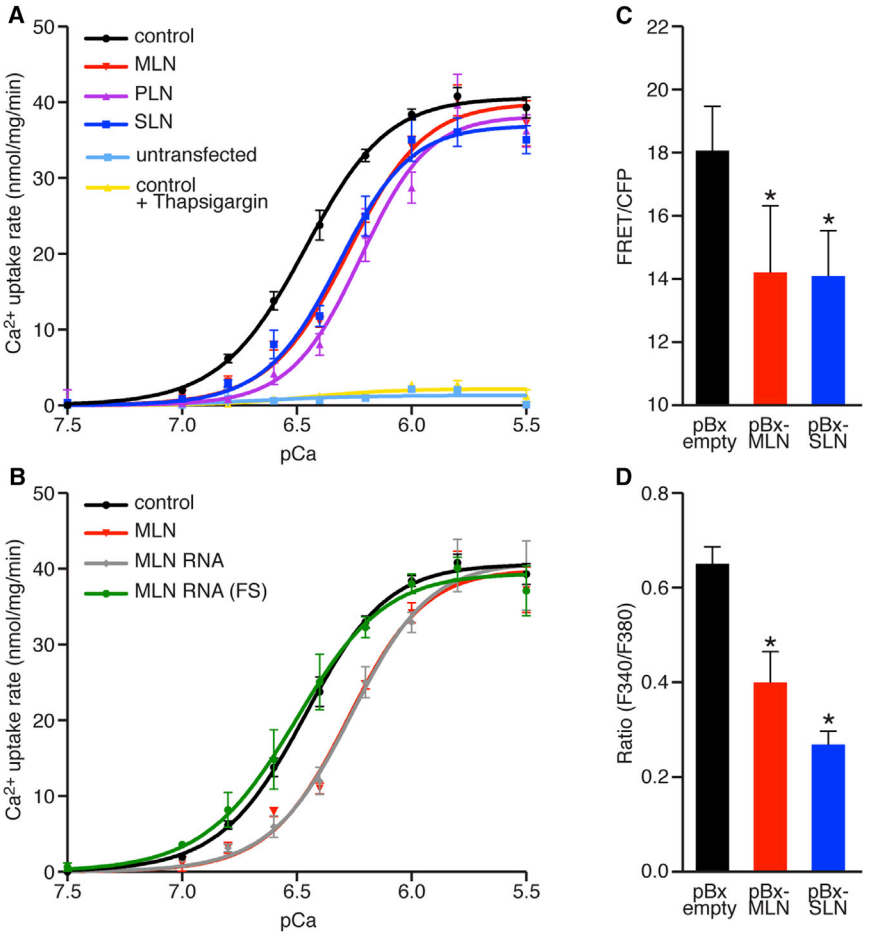

Figure 3. MLN Regulates SR Ca^{2+} Levels by Inhibiting SERCA Pump Activity

(A and B) The Ca^{2+} dependence of the relative rate of Ca^{2+} uptake is shown for homogenates from HEK293 cells cotransfected with SERCA1 and the indicated constructs. Cotransfection with MLN, PLN, or SLN resulted in a similar decrease in Ca^{2+} uptake, corresponding to a decreased affinity of SERCA for Ca^{2+}, relative to empty vector (Control). For comparison, untransfected cells and SERCA1-expressing cells treated with the SERCA inhibitor thapsigargin (100 nM) are shown. The activity of the full-length RNA transcript encoding the MLN ORF (MLN RNA) is abolished by a frameshift mutation in the MLN ORF (MLN-RNA FS).

(C) Retroviral cotransduction of C2C12 myoblasts with the FRET-based Ca^{2+} sensor T1ER with MLN or SLN was used to directly measure the relative levels of SR Ca^{2+}. Both MLN and SLN significantly decreased SR Ca^{2+} levels relative to an empty retroviral vector.

(D) Retroviral overexpression of MLN or SLN in C2C12 myoblasts treated with 4-CMC and imaged with fura-2-AM showed decreased levels of SR Ca^{2+}, measured by peak Ca^{2+} release from the SR.

Data are presented as mean ± SEM (*$p < 0.05$ compared to pBx-empty). See also Table S1.

of identically conserved residues in their transmembrane regions, which are also found in the invertebrate ortholog, sarcolamban (SCL) (Figure 2A) (Magny et al., 2013). Structural modeling of the transmembrane helices showed that all four peptides are predicted to form alpha helical structures with residues arranged in a similar spatial pattern (Figure 2B). PLN and SLN both interact with SERCA in the membrane of the SR in a common groove formed by the M2, M6, and M9 helices of SERCA (Figure 2C) (Toyoshima et al., 2003, 2013; Winther et al., 2013). Automated protein docking of the transmembrane model of MLN with the crystal structure of SERCA revealed that MLN aligned in the same groove that is occupied by PLN and SLN (Figure 2C).

MLN Is Embedded in the SR Membrane and Colocalizes with SERCA1

To examine the subcellular localization of MLN in vivo, we electroporated a plasmid encoding GFP fused to MLN (GFP-MLN) into the flexor digitorum brevis muscle of adult mice. Two-photon laser scanning confocal microscopy allowed for the simultaneous detection of GFP fluorescence and second harmonic generation (SHG) to visualize the myosin A band of the sarcomeres (Nelson et al., 2013). The GFP-MLN fusion protein localized in a repeating pattern that alternated with the myosin A band and overlapped with the localization of an mCherry-SERCA1 fusion protein within the SR (Figure 2D). This pattern was consistent with the localization of GFP-PLN and GFP-SLN fusion proteins (Figure S2C). Additionally, an N-terminal HA-tagged MLN fusion protein (HA-MLN) expressed in C2C12 myoblasts was enriched in the subcellular fraction containing SR/ER membrane proteins (Figure 2E), altogether suggesting that MLN functions in the membrane of the SR.

In coimmunoprecipitation experiments, the HA-MLN fusion protein formed a stable complex with SERCA1 (skeletal muscle specific), SERCA2a (cardiac and slow skeletal muscle specific), and SERCA2b (ubiquitous) isoforms (Figure S2D). Alanine mutagenesis of MLN residues shared with PLN and SLN (L29A, F30A, and F33A) abolished the ability of MLN to interact with SERCA1, whereas mutation of charged residues (K27A, D35A) did not alter this interaction (Figure 2F). These findings suggest that MLN, PLN, and SLN share a common hydrophobic binding motif that stabilizes their association with SERCA.

MLN Regulates Ca^{2+} Handling by Inhibiting SERCA Pump Activity

PLN and SLN both function to inhibit Ca^{2+} reuptake into the SR by lowering the affinity of SERCA for Ca^{2+}, without altering the maximal rate of Ca^{2+} pump activity (V_{max}). To determine if MLN regulates SERCA activity in a similar manner, we directly measured Ca^{2+}-dependent Ca^{2+}-ATPase activity in homogenates from HEK293 cells expressing SERCA1 (Figure 3A). Similar to the effects of PLN and SLN, expression of

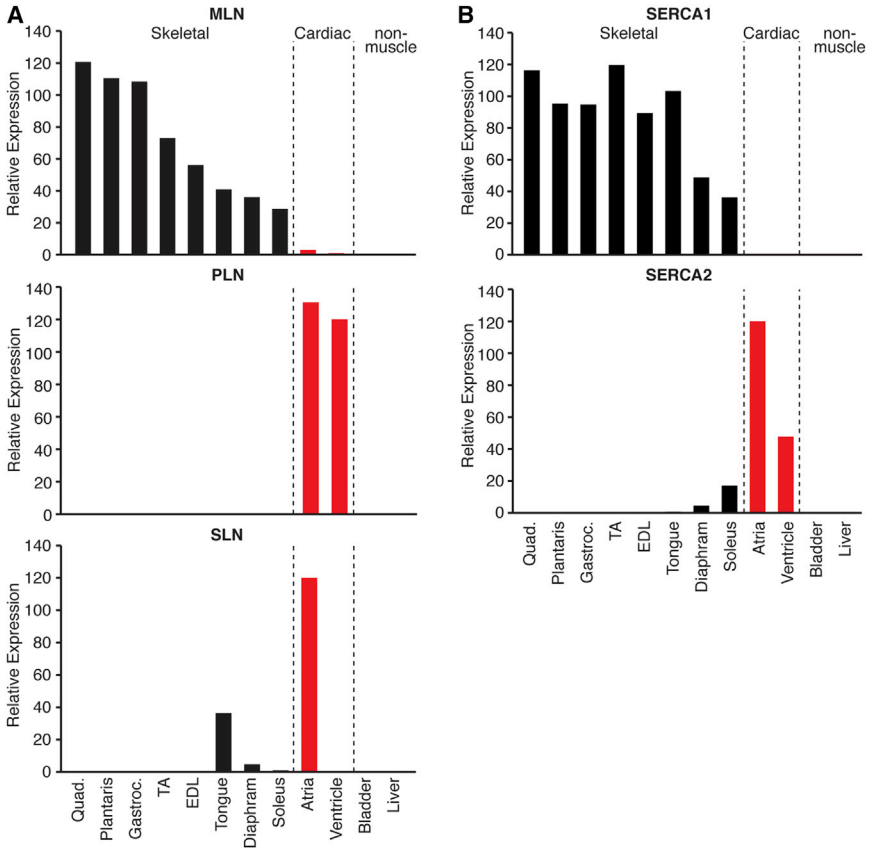

Figure 4. Developmental and Adult Expression of MLN, PLN, and SLN in the Mouse

(A and B) Real-time PCR showing the relative expression of MLN, PLN, SLN, and SERCA isoforms across multiple skeletal muscles, cardiac, and nonmuscle tissues isolated and pooled from three adult 8-week-old C57Bl/6 male mice. See also Figure S3.

MLN caused a significant reduction in the rate of Ca^{2+} uptake, measured as an increase in K_{Ca} (Figure 3A; Table S1). Coexpression of the full-length RNA encoding MLN (MLN RNA) resulted in a similar decrease in Ca^{2+} uptake compared to a vector containing only the MLN coding sequence (Figure 3B). The activity of the MLN RNA was abolished by introduction of a frameshift mutation to disrupt the expression of the MLN micropeptide (MLN-RNA-FS), demonstrating that the RNA itself does not inhibit SERCA activity (Figure 3B). No effects on V_{max} were observed under any conditions tested, and the addition of thapsigargin, a potent inhibitor of SERCA activity, abolished Ca^{2+} uptake (Figure 3A).

Because the concentration of SR Ca^{2+} is dependent upon SERCA reuptake activity, we examined if MLN overexpression could alter SR Ca^{2+} levels in C2C12 myoblasts. SR Ca^{2+} levels were directly measured using retroviral delivery of the fluorescence resonance energy transfer (FRET)-based, SR-localized Ca^{2+} sensor T1ER, using culture conditions previously shown to be sensitive to changes in endogenous SERCA activity (Brandman et al., 2007). Coexpression of MLN or SLN significantly decreased the levels of SR Ca^{2+}, measured as a decrease in T1ER FRET (Figure 3C). We alternatively compared SR Ca^{2+} levels using the ratiometric Ca^{2+} indicator dye fura-2-AM, following SR Ca^{2+} release using the RyR agonist 4-chloro-m-cresol (4-CMC) (Figure 3D). Consistent with our previous findings, overexpression of MLN or SLN significantly decreased peak Ca^{2+} release from the SR (Figure 3D). Together, these findings demonstrate that MLN inhibits SERCA pump kinetics similar to PLN and SLN.

MLN, PLN, and SLN Are Expressed in Different Striated Muscle Types

The structural and functional similarities between MLN, PLN, and SLN suggest they comprise a family of micropeptides that regulate Ca^{2+} handling through modulation of SERCA activity. To determine if PLN or SLN are functionally redundant with MLN in vivo, we examined their expression during developmental and adult stages. In the heart, PLN expression was detectable in both the atria and ventricles, whereas SLN expression was specific to the atria (Figures 4A and S3A). SLN overlapped with the expression of MLN in fetal skeletal muscles, which display a slow phenotype during embryonic development (Figure S3A) (Lu et al., 1999). Consistent with previous reports, quantitative real-time PCR and RNA sequencing (RNA-seq) expression analyses revealed that SLN was markedly downregulated in most adult skeletal muscles, which convert to fast type in the mouse (Figures 4A and S3B) (Tupling et al., 2011). In contrast, MLN was robustly expressed in all adult skeletal muscles, similar to the expression pattern of SERCA1 (Figures 4A and 4B). The expression patterns of PLN and SLN were more similar to the expression of SERCA2, which is highly expressed in cardiac and slow skeletal muscles (Figure 4B). In addition, comparison of RNA-seq expression data revealed that PLN and SLN are not expressed in differentiated C2C12 myotubes, whereas MLN transcripts are robustly expressed (Figure S3C). Thus, MLN, PLN, and SLN are differentially expressed across vertebrate muscle types, and MLN is the most abundant of the three micropeptides expressed in adult skeletal muscle of the mouse.

Transcriptional Control of MLN Expression by MyoD and MEF2

MLN and the skeletal muscle-specific isoforms of SERCA and RyR are coregulated by MyoD, suggesting they comprise a core genetic module important for Ca^{2+} handling in skeletal muscle (Fong et al., 2012). Analysis of the 5′ flanking region of the MLN gene revealed highly conserved binding sites for the myogenic transcription factors MyoD (E-box) and MEF2 (Figure S4A), which bound specifically to these sequences in gel

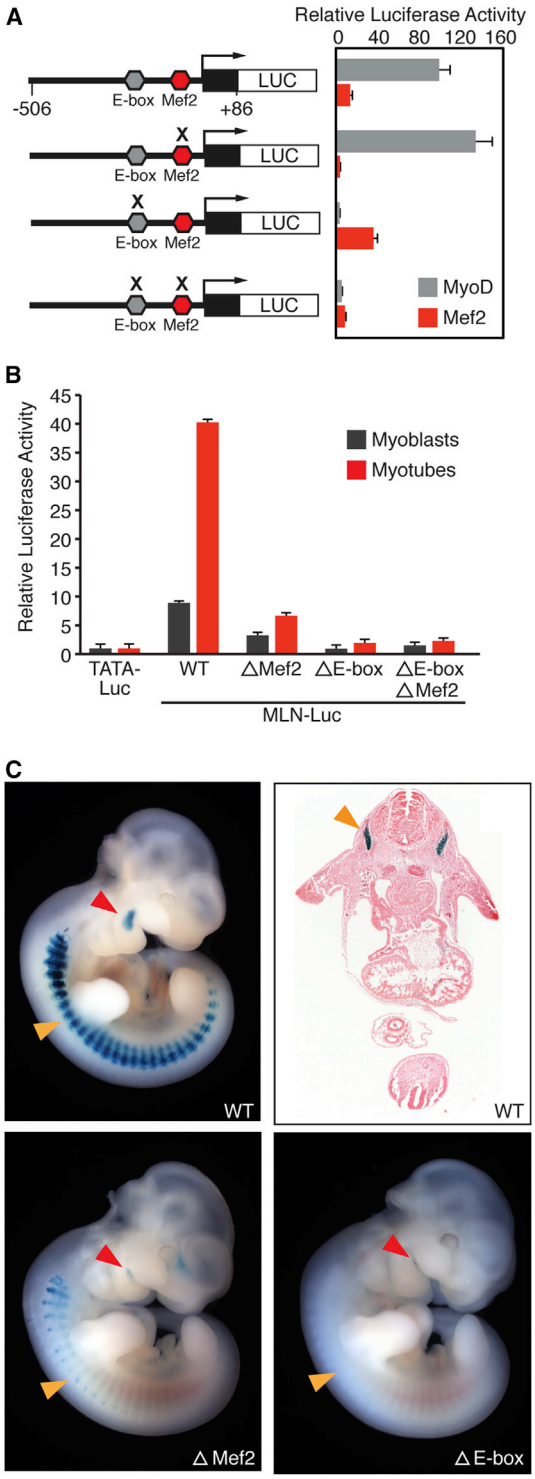

Figure 5. Regulation of MLN Transcription by MyoD and MEF2

(A) A fragment of the MLN promoter (−506 to +86, relative to the transcriptional start site) containing a highly conserved MyoD E-box (CACCTG) and MEF2 site (CTAATAACAG) was cloned in front of the luciferase reporter gene (MLN-Luc). The MLN-Luc reporter was robustly transactivated by the skeletal muscle transcription factors MyoD and MEF2 in COS7 cells (gray and red bars, respectively). Mutation of the E-box (acCCgt) or Mef2 site (CTgggAACAG) (indicated by an X) abrogated transactivation by MyoD:E12 heterodimer or Mef2c, respectively. All luciferase values were normalized to the transactivation of a basal luciferase reporter (TATA-Luc) with MyoD or Mef2, respectively. Data are presented as mean ± SEM.

(B) Luciferase reporter assays showing that MEF2 and E-box enhancer binding sites are essential for transactivation of the MLN promoter in C2C12 myoblasts and myotubes. Data are presented as mean ± SEM.

(C) X-gal and H&E staining of E10.5 mouse embryos harboring either the MLN promoter-lacZ transgene (WT) or mutations in the MLN promoter (ΔMef2 or ΔE-box). The MLN promoter showed expression in the myotomal compartment of the somites (orange arrow) and premyogenic cells in the mandibular arch (red arrow). Mutation of the MEF2 or E-box sequences in the MLN promoter-lacZ transgene abrogated or abolished muscle-specific expression. See also Figure S4.

mobility shift assays (Figure S4B). MyoD and MEF2 independently activated a luciferase reporter linked to the proximal MLN promoter (MLN-Luc), and transactivation was lost upon mutagenesis of their respective binding sites (Figure 5A). Chromatin immunoprecipitation sequencing (ChIP-seq) data at this locus revealed that MyoD bound specifically to this region in both C2C12 myoblasts and myotubes (Figure S4C) (Bernstein et al., 2012). The activity of the MLN-Luc promoter in C2C12 myoblasts and myotubes was similarly dependent upon both the MEF2 and E-box sequences, which, when mutated, resulted in the loss and abrogation of MLN promoter activation, respectively (Figure 5B). Consistent with this, a LacZ transgene controlled by the MLN promoter (MLN-lacZ) displayed skeletal muscle-specific expression in vivo and was dependent upon the MEF2 and E-box sequences for full promoter activation (Figure 5C). Thus, the MLN gene is a direct target of the core transcription factors that activate skeletal myogenesis.

Generation of MLN Knockout Mice Using TALENs

To investigate the function of MLN in vivo, we generated MLN knockout (KO) mice using TAL effector nuclease (TALEN)-mediated homologous recombination. A unique TALEN pair specific for exon 1 of the MLN locus was designed and constructed using the REAL assembly method (Reyon et al., 2012). A loss-of-function allele was created using a donor plasmid to insert a red fluorescent reporter (tdTomato), followed by a triple polyadenylation cassette into exon 1 in the MLN locus (Figure 6A). This strategy was designed to prematurely terminate transcription upstream of the MLN coding sequence but allow for the expression of a red fluorescent reporter by the endogenous MLN promoter. Correct targeting was verified by Southern blot and PCR-based genotyping (Figures 6B and S5A). Detection of tdTomato fluorescence in MLN KO mice was specific to skeletal muscle and was not detected in other tissues (Figure 6C). qPCR using primer pairs specific to the downstream exons 2 and 3 demonstrated that the MLN transcript was absent in skeletal muscle from MLN KO mice (Figure 6D).

MLN KO mice were born at expected Mendelian ratios from heterozygous intercrosses and showed no obvious morphological abnormalities or differences in body or muscle weights (Figure S5B). Mice lacking PLN and SLN also have nonpathological phenotypes but show enhanced Ca^{2+} handling and contractility in cardiac and slow skeletal muscle (Luo et al., 1994; MacLennan and Kranias, 2003; Tupling et al., 2011).

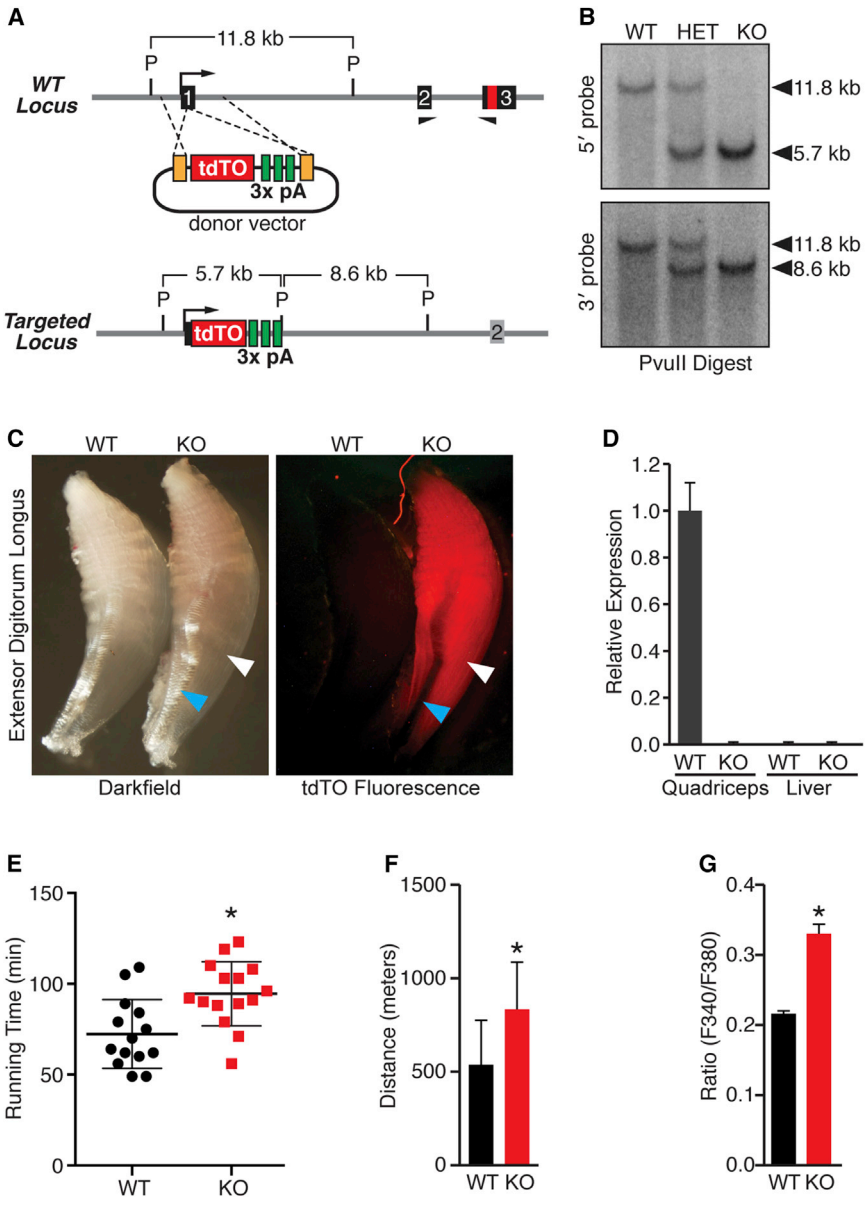

Figure 6. Generation and Characterization of MLN Knockout Mice

(A) TALEN-mediated homologous recombination was used to insert a tdTomato fluorescent reporter and triple polyadenylation cassette into exon 1 of the MLN locus to generate a null allele. A schematic of the donor vector and targeting strategy is shown. P, PvuII.

(B) Southern blot analysis confirming correct targeting of the tdTO-triple polyadenylation cassette into exon 1 of the MLN locus using probes 5′ and 3′ to the TALEN cut site.

(C) tdTomato fluorescence was specific to skeletal muscle (white arrowhead) of MLN KO mice and not detected in other tissues, such as tendon (blue arrowhead).

(D) Real-time PCR using primers specific to exons 2 and 3 demonstrating absence of MLN transcripts in MLN KO muscle, as well as in liver.

(E) Muscle performance was measured using forced treadmill running to exhaustion. MLN KO (n = 15) mice ran ~31% longer than WT littermates (n = 14).

(F) Comparison of distance run by MLN KO and WT mice in Figure 6E.

(G) Myoblasts isolated and cultured from MLN KO hindlimb muscles were imaged using Fura-2-AM and treated with the RyR agonist 4-CMC in the absence of extracellular Ca^{2+} to indirectly measure SR Ca^{2+} levels. MLN KO myoblasts showed significantly increased SR Ca^{2+} levels, measured as peak Ca^{2+} release from the SR. Data are presented as mean ± SEM (*$p < 0.05$ compared to WT as in E and F and pBx-empty in G).

See also Figure S5.

Enhanced Ca^{2+} Handling and Skeletal Muscle Performance in MLN KO Mice

To examine the potential role of MLN in regulating skeletal muscle performance, we subjected 8-week-old wild-type (WT) and MLN KO mice to a regimen of forced treadmill running to exhaustion. Remarkably, MLN KO mice ran an average time of ~31% longer than their WT littermates, representing a 55% increase in running distance (Figures 6E and 6F). Mice with a fast-to-slow fiber type switch also show increased running performance (van Rooij et al., 2009). However, histological analyses of hindlimb muscles, including quadriceps (fast-type) and soleus (slow-type) muscles revealed no obvious differences in fiber-type identity or myofiber size between WT and MLN KO mice (Figures S5C–S5E), indicating that MLN functions through a different mechanism to regulate muscle performance.

Next, we investigated whether SR Ca^{2+} levels were altered in primary myoblasts isolated from hindlimb muscles of MLN KO versus WT littermates. SR Ca^{2+} levels were measured using the calcium indicator fura-2-AM and SR Ca^{2+} release by the addition of the RyR agonist 4-CMC. Strikingly, MLN KO myoblasts showed significantly increased SR Ca^{2+} levels compared to WT myoblasts, measured as peak SR Ca^{2+} release (Figure 6G). This increase occurred without changes in the expression of RyR1 and SERCA1 expression between WT and MLN KO muscles (Figure S5F), consistent with the function of MLN as an inhibitor of SERCA activity. Together, these findings support the function of MLN as the dominant regulator of SERCA activity in adult skeletal muscle.

DISCUSSION

SERCA is a key regulator of striated muscle performance by serving as the major Ca^{2+} ATPase responsible for the reuptake of cytosolic Ca^{2+} into the SR (Figure 7A). Direct modulation of SERCA pump activity by the micropeptides PLN and SLN regulates muscle contractility by diminishing the rate of Ca^{2+} reuptake into the SR. However, because PLN and SLN are not

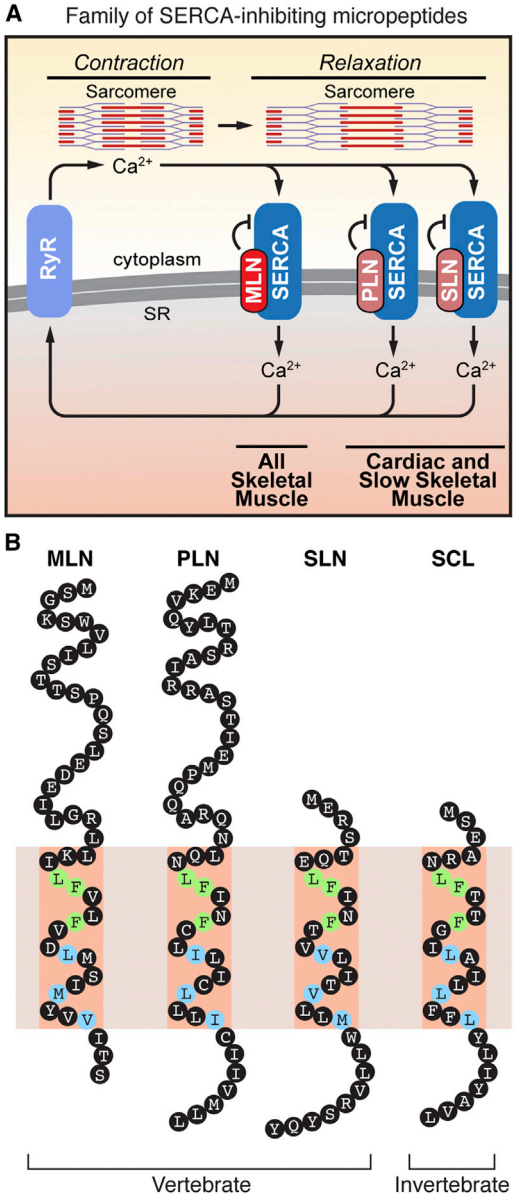

Figure 7. A Family of SERCA-Inhibitory Micropeptides

(A) RyR and SERCA play a critical role in muscle contractility by controlling Ca^{2+} cycling between the cytosol and SR. MLN, PLN, and SLN inhibit SERCA pump activity in different striated muscle types of vertebrates.

(B) Illustration of the family of SERCA-inhibitory micropeptides. The discovery of MLN reveals that vertebrates encode three SERCA inhibitory peptides that share conserved residues within their transmembrane alpha helices. Green shading denotes identical residues, and blue shading denotes similar residues. MLN, myoregulin; PLN, phospholamban; SLN, sarcolipin; SCL, sarcolamban.

expressed in most adult skeletal muscles of mice, the possible existence of other SERCA regulatory factors has remained an open question.

Our biochemical and in vivo results show that MLN forms a stable complex with SERCA in the membrane of the SR and that MLN directly influences SR Ca^{2+} levels and maximal exercise performance. The robust skeletal muscle-specific expression of MLN, resulting from direct transactivation by the myogenic transcription factors MyoD and MEF2, further highlight MLN as the predominant SERCA regulating micropeptide in adult skeletal muscle. The discovery of MLN reveals a universal mechanism for the control of SERCA activity by a family of related micropeptides expressed in different striated muscle types in vertebrates (Figure 7A).

Micropeptides Can Be Concealed within RNAs Misannotated as Noncoding

Micropeptides remain highly underrepresented in genome annotations due in large part to the difficulty in identifying functional short ORFs in RNA transcripts. Recent advances in bioinformatic and biochemical methodologies have revealed that lncRNAs may harbor concealed micropeptides; however, only a few have been functionally verified and characterized in vivo. Here, we have identified and characterized the function of a conserved micropeptide in vertebrates that functions as an important regulator of skeletal muscle performance through modulation of Ca^{2+} handling by SERCA. Given the attention that has been focused on the control of SERCA activity and muscle function over the years, it is remarkable that such a key regulator of these processes has gone undetected. Undoubtedly, this is because the MLN ORF is concealed in an RNA annotated as noncoding. Our discovery of MLN was possible due to its high sequence conservation in vertebrates and the presence of an identifiable functional domain, a type II transmembrane alpha helix. We found that the MLN alpha helix shares residues in common with PLN and SLN; however, common bioinformatic search tools alone are not sufficient to identify the relatedness of MLN, PLN, and SLN. Interestingly, both PLN and SLN were first discovered as micropeptides and subsequently mapped to RNA transcripts (Kirchberber et al., 1975; Wawrzynow et al., 1992). The PLN and SLN genes share a genomic architecture similar to that of MLN, in which the small ORFs are encoded in the 5′ region of the terminal exon. Indeed, the transcripts encoding PLN and SLN may have also been annotated as noncoding, if not for their prior discovery as micropeptides.

A Family of SERCA-Inhibitory Micropeptides

In *Drosophila*, the invertebrate ortholog of SERCA is encoded by a single gene (Ca-P60A) and is modulated by the recently identified micropeptide sarcolamban (SCL) (Magny et al., 2013). In vertebrates, the SERCA family has expanded to encode three genes (SERCA1-3) that give rise to multiple alternate splice variants with differing kinetic properties and expression patterns (Anger et al., 1994; Periasamy and Kalyanasundaram, 2007). The expansion of vertebrate gene families occurred through whole-genome and gene-duplication events, resulting in the formation of paralogous gene families. Combined with the tissue-specific expression patterns of the individual SERCA isoforms, the differential expression of MLN, PLN, and SLN likely contributes to the unique Ca^{2+} handling and contractile properties of different striated muscle types in vertebrates. In addition, the extent to which MLN, PLN, and SLN partially overlap in their expression in different muscle types may influence the calcium kinetics and performance of these tissues. Coexpression of

PLN and SLN in atrial cardiomyocytes and slow skeletal muscle has been shown to result in the superinhibition of SERCA pump activity (MacLennan et al., 2003). MLN expression overlaps with that of PLN and SLN in adult slow skeletal muscle and with SLN in developing skeletal muscles. Future biochemical and animal studies are required to determine the extent to which MLN synergizes with PLN and SLN in coregulating SERCA activity in slow-type and developing skeletal muscle. SLN expression in larger animals is more widespread than in rodents, occurring in both fast- and slow-type muscles (Fajardo et al., 2013; Odermatt et al., 1997). A synergistic interaction between MLN and SLN may be more biologically relevant in the adult tissues of these species; however, the relative expression patterns of these two genes in these species remain to be determined.

Apart from spatiotemporal differences in expression, the SERCA-regulatory peptides differ in size and presence of additional secondary structures. A schematic illustration of the family of SERCA-inhibitory micropeptides is shown in Figure 7B. Both SLN and SCL lack extended N-terminal regions and additional secondary structures other than their transmembrane alpha helices. MLN and PLN have expanded N-terminal cytoplasmic regions that encode a beta sheet and alpha helix, respectively. The N-terminal sequence of PLN has been shown to be critical for its function, and phosphorylation of serine-16 by protein kinase A (PKA) or threonine-17 by Ca^{2+}/calmodulin-dependent protein kinase II (CaMKII) diminishes the ability of PLN to inhibit SERCA activity (Mattiazzi et al., 2006; Wegener et al., 1989). The N-terminal sequence of MLN could serve as a similar regulatory domain through phosphorylation, as this sequence contains multiple serine and threonine residues. Deciphering the physiological signaling pathways that regulate MLN expression and function will be important to fully understand its role in skeletal muscle development and disease.

Future Questions

Defects in Ca^{2+} signaling underlie the pathogenesis of many muscle diseases that arise from mutations in components of Ca^{2+} signaling pathways, as well as diseases that arise from a loss of myofiber structural integrity (Berchtold et al., 2000; Millay et al., 2008). Given the importance of SERCA pump activity in regulating Ca^{2+} handling and the pathogenesis of skeletal muscle diseases, such as Brody myopathy and muscular dystrophies (Allen et al., 2010; Goonasekera et al., 2011; Odermatt et al., 1996), the discovery of MLN opens interesting possibilities for the modulation of these pathways. Considering the enhanced exercise capacity of MLN KO mice, it is interesting to speculate that pharmacologic approaches to disrupt the association of MLN with SERCA might have similar salutary effects. Modulation of SERCA activity in skeletal muscle has also been implicated in the control of systemic energy homeostasis (Bal et al., 2012), raising the interesting possibility that MLN may exert additional metabolic functions. Considering that SERCA is also important in Ca^{2+} regulation in nonmuscle cell types in which MLN, PLN, and SLN are not expressed, it is interesting to speculate that additional SERCA-modulating micropeptides may be concealed within putative lncRNAs expressed in other tissues. Finally, the discovery of MLN as a previously unrecognized regulator of muscle function suggests that the microproteome, which is largely unexplored, represents a reservoir for future biological insights.

EXPERIMENTAL PROCEDURES

TALEN-Mediated Homologous Recombination in Mice

A unique TALEN pair specific for the MLN locus was designed using the ZiFiT Targeter Program (http://zifit.partners.org/ZiFiT/Introduction.aspx) and constructed using the REAL Assembly Kit (Addgene) (Reyon et al., 2012). A donor vector containing the tdTomato reporter and triple polyadenylation sequences was constructed by incorporating short 5′ and 3′ homology arms specific to the MLN locus. TALEN mRNAs were in vitro transcribed using the mMessage mMachine T7 Ultra Kit (Life Technologies), diluted to 25 ng μl^{-1}, and coinjected with 3 ng μl^{-1} of the circular DNA donor plasmid into the nucleus and cytoplasm of one-cell-stage embryos (B6C3F1) and transferred into pseudopregnant female ICR mice.

Study Approval

All experimental procedures involving animals in this study were reviewed and approved by the University of Texas Southwestern Medical Center's Institutional Animal Care and Use Committee.

Radioisotopic In Situ Hybridization

In situ hybridizations were performed as previously described (Shelton et al., 2000). See the Extended Experimental Procedures for a more detailed protocol. The primer sequences used to clone MLN, PLN, and SLN cDNA templates are listed in Table S2.

CRISPR/Cas9-Mediated Homologous Recombination in C2C12 Myoblasts

A single-guide RNA (sgRNA) specific to the C-terminal coding sequence of the mouse MLN locus was cloned into the sgRNA/Cas9 expression vector px330 (MLN-FLAG-px330). The donor vector was constructed with a single FLAG epitope tag in-frame with the MLN coding sequence flanked by ~500 base pair homology arms specific to the MLN locus. MLN-FLAG knockin clones were generated by transient cotransfection and expanded from single-cell clones. Detection of endogenous MLN-FLAG peptide was performed by immunoblotting with a rabbit anti-FLAG antibody (Sigma) on protein lysates immunoprecipitated with mouse anti-FLAG agarose beads (Sigma).

Treadmill Running

In blinded studies, male MLN KO and WT littermate mice were subjected to forced exercise on a treadmill (Exer-6M, Columbus Instruments, 10% incline) at 8 weeks of age using a regimen previously described (van Rooij et al., 2009). See the Extended Experimental Procedures for a more detailed protocol.

Intracellular Ca^{2+} Imaging

Cytosolic Ca^{2+} levels were measured as described previously (Liou et al., 2005), with the exception that retroviral-transduced C2C12 cells or primary myoblasts were plated on Ibidi μ-35 mm tissue-culture dishes and cultured for 24 hr in low Ca^{2+} (0.1 mM Ca^{2+}) prior to imaging to increase sensitivity to changes in SR Ca^{2+} levels (Brandman et al., 2007). SR Ca^{2+} levels were directly measured using T1ER as previously described (Abell et al., 2011; Tsai et al., 2014). See the Extended Experimental Procedures for a more detailed protocol.

Oxalate-Supported Ca^{2+} Uptake Measurements in HEK293 Lysates

Oxalate-supported Ca^{2+}-dependent Ca^{2+}-ATPase activity in homogenates was measured by a modification of the Millipore filtration technique as described previously (Holemans et al., 2014; Luo et al., 1994). HEK293 cells were cotransfected with equal amounts of an expression plasmid encoding mouse SERCA1 and an expression plasmid encoding MLN, PLN, or SLN. See the Extended Experimental Procedures for a more detailed protocol.

Coimmunoprecipitations and Western Blot Analysis

Coimmunoprecipitations (coIPs) were performed as previously described (Anderson et al., 2009). Tris-tricine-SDS-PAGE was carried out using 16.5%

Tris-tricine gels (BioRad) and Tris-tricine-SDS running buffer (BioRad). See the Extended Experimental Procedures for a more detailed protocol.

Real-Time PCR

Total RNA was prepared from whole muscles using Trizol (Invitrogen) and treated with DNase prior to reverse transcription by Superscript III (Invitrogen). Real-time PCR was performed using TaqMan probes (ABI) or SYBR green using primers in Table S2. TaqMan probes include Mck (Mm00432556_m1), Mef2c (Mm01340842_m1), SLN (Mm00481536_m1), PLN (Mm00452263_m1), and SERCA2 (Mm01201434_m1). Primers for SYBR green reactions are listed in Table S2.

Electrophoretic Mobility Shift Assays

Electrophoretic mobility shift assays (EMSAs) were performed as previously described (Anderson et al., 2012) using recombinant myc-tagged proteins expressed in COS7 cells and double-stranded EMSA probes created by annealing complementary oligonucleotides. Probe sequences are listed in Table S2. Supershifts were performed by adding 1 μg of mouse anti-Myc antibody (Invitrogen). See the Extended Experimental Procedures for a more detailed protocol.

Luciferase Assays

Luciferase assays were performed as previously described (Anderson et al., 2009). Luciferase activity was measured using a FluoStar OPTIMA microplate reader (BMG Labtech) and normalized to beta-galactosidase activity using the FluoReporter LacZ/Galactosidase Quantitation Kit (Invitrogen). See the Extended Experimental Procedures for a more detailed protocol.

Subcellular Fractionation

C2C12 myoblasts infected with a retrovirus encoding the HA-MLN fusion protein (pBabeX-HA-MLN) were fractionated as previously described (Millay et al., 2013). See the Extended Experimental Procedures for a more detailed protocol.

Northern and Southern Blot Analysis

Northern blots were performed using a commercially prepared adult mouse multitissue RNA blot (MN-MT-1; Zyagen) hybridized with a radiolabeled DNA probe specific to the full-length MLN transcript. Radiolabeled DNA probes for northern and Southern blots were generated using a RadPrime Kit (Invitrogen) (Table S2).

Histology and Immunohistochemistry

Skeletal muscle tissues were dissected and fixed overnight in 4% formaldehyde in PBS prior to paraffin embedding and sectioning using routine procedures. Immunohistochemistry was performed on deparaffinized sections using a HistoMouse-Plus kit (Invitrogen) using primary antibodies specific to fast (MY32; Sigma) and slow (NOQ7.54; Sigma) myosins. Wheat germ agglutinin (WGA) staining was performed using Alexa Fluor 555-conjugated WGA (Invitrogen) as described previously (Liu et al., 2011).

Analysis of RNA-Seq Expression Data

Raw data for C2C12 cells and triceps brachii muscle were downloaded from the Short Read Archive (SRP002119 and SRP008123, respectively). Reads were mapped to the UCSC mm9 genome annotation using TopHat, and alignments were processed to bigWig coverage maps and viewed using the UCSC genome browser.

Circular Dichroism Spectroscopy

Circular dichroism (CD) spectroscopy measurements were performed using a JASCO J-815 spectrometer on in vitro-synthesized full-length MLN (Peptide 2.0). The secondary structure elements were calculated using Yang's fit. The root-mean-square deviation for the observed and calculated CD spectra values was 3%. See the Extended Experimental Procedures for a more detailed protocol.

Structural Modeling and Automated Protein Docking

The helical domains of MLN, PLN, SLN, and SCL were created ab initio using I-TASSER (Zhang, 2008). Automated protein docking of the MLN model with the crystal structure of SERCA1 (4H1W) was performed using ClusPro 2.0 (Comeau et al., 2004).

Adult Muscle Electroporation and Imaging

Flexor digitorum brevis (FDB) muscles of 12-week-old male mice were electroporated as previously described (Nelson et al., 2013), with expression vectors encoding N-terminal GFP fusions to MLN, PLN, or SLN. Unfixed FDB muscles were examined directly using two-photon laser scanning microscopy (Zeiss; LSM 780), with reverse second harmonic generation to visualize the A bands as an internal reference. See the Extended Experimental Procedures for a more detailed protocol.

SUPPLEMENTAL INFORMATION

Supplemental Information includes Extended Experimental Procedures, five figures, and two tables and can be found with this article online at http://dx.doi.org/10.1016/j.cell.2015.01.009.

ACKNOWLEDGMENTS

We thank Dr. Tobias Meyer at Stanford University Medical Center for generously providing the pcDNA-T1ER vector and Dr. David H. MacLennan at University of Toronto for generously providing the Serca1 (A52) antibody. This work was supported by grants from the NIH (HL-077439, HL-111665, HL-093039, DK-099653, and U01-HL-100401), Fondation Leducq Networks of Excellence, and the Robert A. Welch Foundation (grant 1-0025 to E.N.O.; I-1789 to J.L.). D.M.A. was supported by an American Heart Association postdoctoral fellowship (13POST14570050). K.M.A. was supported by an American Heart Association predoctoral fellowship (14PRE19830031). B.R.N. was supported by an NIH Training grant (1F30AR067094-01), and P.K. was supported by a postdoctoral grant from the Sigrid Juselius Foundation.

Received: August 19, 2014
Revised: November 24, 2014
Accepted: January 5, 2015
Published: January 29, 2015

REFERENCES

Abell, E., Ahrends, R., Bandara, S., Park, B.O., and Teruel, M.N. (2011). Parallel adaptive feedback enhances reliability of the Ca2+ signaling system. Proc. Natl. Acad. Sci. USA *108*, 14485–14490.

Allen, D.G., Gervasio, O.L., Yeung, E.W., and Whitehead, N.P. (2010). Calcium and the damage pathways in muscular dystrophy. Can. J. Physiol. Pharmacol. *88*, 83–91.

Anderson, D.M., Beres, B.J., Wilson-Rawls, J., and Rawls, A. (2009). The homeobox gene Mohawk represses transcription by recruiting the sin3A/HDAC co-repressor complex. Dev. Dyn. *238*, 572–580.

Anderson, D.M., George, R., Noyes, M.B., Rowton, M., Liu, W., Jiang, R., Wolfe, S.A., Wilson-Rawls, J., and Rawls, A. (2012). Characterization of the DNA-binding properties of the Mohawk homeobox transcription factor. J. Biol. Chem. *287*, 35351–35359.

Andrews, S.J., and Rothnagel, J.A. (2014). Emerging evidence for functional peptides encoded by short open reading frames. Nat. Rev. Genet. *15*, 193–204.

Anger, M., Samuel, J.L., Marotte, F., Wuytack, F., Rappaport, L., and Lompré, A.M. (1994). In situ mRNA distribution of sarco(endo)plasmic reticulum Ca(2+)-ATPase isoforms during ontogeny in the rat. J. Mol. Cell. Cardiol. *26*, 539–550.

Bal, N.C., Maurya, S.K., Sopariwala, D.H., Sahoo, S.K., Gupta, S.C., Shaikh, S.A., Pant, M., Rowland, L.A., Bombardier, E., Goonasekera, S.A., et al. (2012). Sarcolipin is a newly identified regulator of muscle-based thermogenesis in mammals. Nat. Med. *18*, 1575–1579.

Bassel-Duby, R., and Olson, E.N. (2006). Signaling pathways in skeletal muscle remodeling. Annu. Rev. Biochem. *75*, 19–37.

Bazzini, A.A., Johnstone, T.G., Christiano, R., Mackowiak, S.D., Obermayer, B., Fleming, E.S., Vejnar, C.E., Lee, M.T., Rajewsky, N., Walther, T.C., and Giraldez, A.J. (2014). Identification of small ORFs in vertebrates using ribosome footprinting and evolutionary conservation. EMBO J. *33*, 981–993.

Berchtold, M.W., Brinkmeier, H., and Müntener, M. (2000). Calcium ion in skeletal muscle: its crucial role for muscle function, plasticity, and disease. Physiol. Rev. *80*, 1215–1265.

Bernstein, B.E., Birney, E., Dunham, I., Green, E.D., Gunter, C., and Snyder, M.; ENCODE Project Consortium (2012). An integrated encyclopedia of DNA elements in the human genome. Nature *489*, 57–74.

Berridge, M.J., Bootman, M.D., and Roderick, H.L. (2003). Calcium signalling: dynamics, homeostasis and remodelling. Nat. Rev. Mol. Cell Biol. *4*, 517–529.

Brandman, O., Liou, J., Park, W.S., and Meyer, T. (2007). STIM2 is a feedback regulator that stabilizes basal cytosolic and endoplasmic reticulum Ca2+ levels. Cell *131*, 1327–1339.

Briggs, F.N., Lee, K.F., Wechsler, A.W., and Jones, L.R. (1992). Phospholamban expressed in slow-twitch and chronically stimulated fast-twitch muscles minimally affects calcium affinity of sarcoplasmic reticulum Ca(2+)-ATPase. J. Biol. Chem. *267*, 26056–26061.

Chu, G., Ferguson, D.G., Edes, I., Kiss, E., Sato, Y., and Kranias, E.G. (1998). Phospholamban ablation and compensatory responses in the mammalian heart. Ann. N Y Acad. Sci. *853*, 49–62.

Comeau, S.R., Gatchell, D.W., Vajda, S., and Camacho, C.J. (2004). ClusPro: an automated docking and discrimination method for the prediction of protein complexes. Bioinformatics *20*, 45–50.

Dorn, G.W., 2nd, and Molkentin, J.D. (2004). Manipulating cardiac contractility in heart failure: data from mice and men. Circulation *109*, 150–158.

Fajardo, V.A., Bombardier, E., Vigna, C., Devji, T., Bloemberg, D., Gamu, D., Gramolini, A.O., Quadrilatero, J., and Tupling, A.R. (2013). Co-expression of SERCA isoforms, phospholamban and sarcolipin in human skeletal muscle fibers. PLoS ONE *8*, e84304.

Fong, A.P., Yao, Z., Zhong, J.W., Cao, Y., Ruzzo, W.L., Gentleman, R.C., and Tapscott, S.J. (2012). Genetic and epigenetic determinants of neurogenesis and myogenesis. Dev. Cell *22*, 721–735.

Goonasekera, S.A., Lam, C.K., Millay, D.P., Sargent, M.A., Hajjar, R.J., Kranias, E.G., and Molkentin, J.D. (2011). Mitigation of muscular dystrophy in mice by SERCA overexpression in skeletal muscle. J. Clin. Invest. *121*, 1044–1052.

Holemans, T., Vandecaetsbeek, I., Wuytack, F., and Vangheluwe, P. (2014). Measuring Ca2+-dependent Ca2+-uptake activity in the mouse heart. Cold Spring Harb Protoc *2014*, 876–886.

Kirchberber, M.A., Tada, M., and Katz, A.M. (1975). Phospholamban: a regulatory protein of the cardiac sarcoplasmic reticulum. Recent Adv. Stud. Cardiac Struct. Metab. *5*, 103–115.

Kranias, E.G., and Hajjar, R.J. (2012). Modulation of cardiac contractility by the phospholamban/SERCA2a regulatome. Circ. Res. *110*, 1646–1660.

Liou, J., Kim, M.L., Heo, W.D., Jones, J.T., Myers, J.W., Ferrell, J.E., Jr., and Meyer, T. (2005). STIM is a Ca2+ sensor essential for Ca2+-store-depletion-triggered Ca2+ influx. Curr. Biol. *15*, 1235–1241.

Liu, N., Bezprozvannaya, S., Shelton, J.M., Frisard, M.I., Hulver, M.W., McMillan, R.P., Wu, Y., Voelker, K.A., Grange, R.W., Richardson, J.A., et al. (2011). Mice lacking microRNA 133a develop dynamin 2–dependent centronuclear myopathy. J. Clin. Invest. *121*, 3258–3268.

Lu, B.D., Allen, D.L., Leinwand, L.A., and Lyons, G.E. (1999). Spatial and temporal changes in myosin heavy chain gene expression in skeletal muscle development. Dev. Biol. *216*, 312–326.

Luo, W., Grupp, I.L., Harrer, J., Ponniah, S., Grupp, G., Duffy, J.J., Doetschman, T., and Kranias, E.G. (1994). Targeted ablation of the phospholamban gene is associated with markedly enhanced myocardial contractility and loss of beta-agonist stimulation. Circ. Res. *75*, 401–409.

MacLennan, D.H., and Kranias, E.G. (2003). Phospholamban: a crucial regulator of cardiac contractility. Nat. Rev. Mol. Cell Biol. *4*, 566–577.

MacLennan, D.H., Asahi, M., and Tupling, A.R. (2003). The regulation of SERCA-type pumps by phospholamban and sarcolipin. Ann. N Y Acad. Sci. *986*, 472–480.

Magny, E.G., Pueyo, J.I., Pearl, F.M., Cespedes, M.A., Niven, J.E., Bishop, S.A., and Couso, J.P. (2013). Conserved regulation of cardiac calcium uptake by peptides encoded in small open reading frames. Science *341*, 1116–1120.

Mattiazzi, A., Mundiña-Weilenmann, C., Vittone, L., Said, M., and Kranias, E.G. (2006). The importance of the Thr17 residue of phospholamban as a phosphorylation site under physiological and pathological conditions. Braz. J. Med. Biol. Res. *39*, 563–572.

Millay, D.P., Sargent, M.A., Osinska, H., Baines, C.P., Barton, E.R., Vuagniaux, G., Sweeney, H.L., Robbins, J., and Molkentin, J.D. (2008). Genetic and pharmacologic inhibition of mitochondrial-dependent necrosis attenuates muscular dystrophy. Nat. Med. *14*, 442–447.

Millay, D.P., O'Rourke, J.R., Sutherland, L.B., Bezprozvannaya, S., Shelton, J.M., Bassel-Duby, R., and Olson, E.N. (2013). Myomaker is a membrane activator of myoblast fusion and muscle formation. Nature *499*, 301–305.

Minamisawa, S., Wang, Y., Chen, J., Ishikawa, Y., Chien, K.R., and Matsuoka, R. (2003). Atrial chamber-specific expression of sarcolipin is regulated during development and hypertrophic remodeling. J. Biol. Chem. *278*, 9570–9575.

Nelson, B.R., Wu, F., Liu, Y., Anderson, D.M., McAnally, J., Lin, W., Cannon, S.C., Bassel-Duby, R., and Olson, E.N. (2013). Skeletal muscle-specific T-tubule protein STAC3 mediates voltage-induced Ca2+ release and contractility. Proc. Natl. Acad. Sci. USA *110*, 11881–11886.

Odermatt, A., Taschner, P.E., Khanna, V.K., Busch, H.F., Karpati, G., Jablecki, C.K., Breuning, M.H., and MacLennan, D.H. (1996). Mutations in the gene-encoding SERCA1, the fast-twitch skeletal muscle sarcoplasmic reticulum Ca2+ ATPase, are associated with Brody disease. Nat. Genet. *14*, 191–194.

Odermatt, A., Taschner, P.E., Scherer, S.W., Beatty, B., Khanna, V.K., Cornblath, D.R., Chaudhry, V., Yee, W.C., Schrank, B., Karpati, G., et al. (1997). Characterization of the gene encoding human sarcolipin (SLN), a proteolipid associated with SERCA1: absence of structural mutations in five patients with Brody disease. Genomics *45*, 541–553.

Pan, Y., Zvaritch, E., Tupling, A.R., Rice, W.J., de Leon, S., Rudnicki, M., McKerlie, C., Banwell, B.L., and MacLennan, D.H. (2003). Targeted disruption of the ATP2A1 gene encoding the sarco(endo)plasmic reticulum Ca2+ ATPase isoform 1 (SERCA1) impairs diaphragm function and is lethal in neonatal mice. J. Biol. Chem. *278*, 13367–13375.

Periasamy, M., and Kalyanasundaram, A. (2007). SERCA pump isoforms: their role in calcium transport and disease. Muscle Nerve *35*, 430–442.

Reyon, D., Khayter, C., Regan, M.R., Joung, J.K., and Sander, J.D. (2012). Engineering designer transcription activator-like effector nucleases (TALENs) by REAL or REAL-Fast assembly. Curr. Protoc. Mol. Biol. *Chapter 12*, Unit 12. 15.

Rossi, A.E., and Dirksen, R.T. (2006). Sarcoplasmic reticulum: the dynamic calcium governor of muscle. Muscle Nerve *33*, 715–731.

Schmitt, J.P., Kamisago, M., Asahi, M., Li, G.H., Ahmad, F., Mende, U., Kranias, E.G., MacLennan, D.H., Seidman, J.G., and Seidman, C.E. (2003). Dilated cardiomyopathy and heart failure caused by a mutation in phospholamban. Science *299*, 1410–1413.

Shelton, J.M., Lee, M.H., Richardson, J.A., and Patel, S.B. (2000). Microsomal triglyceride transfer protein expression during mouse development. J. Lipid Res. *41*, 532–537.

Slack, J.P., Grupp, I.L., Luo, W., and Kranias, E.G. (1997). Phospholamban ablation enhances relaxation in the murine soleus. Am. J. Physiol. *273*, C1–C6.

Tada, M., and Toyofuku, T. (1998). Molecular regulation of phospholamban function and expression. Trends Cardiovasc. Med. *8*, 330–340.

Toyoshima, C., Asahi, M., Sugita, Y., Khanna, R., Tsuda, T., and MacLennan, D.H. (2003). Modeling of the inhibitory interaction of phospholamban with the Ca2+ ATPase. Proc. Natl. Acad. Sci. USA *100*, 467–472.

Toyoshima, C., Iwasawa, S., Ogawa, H., Hirata, A., Tsueda, J., and Inesi, G. (2013). Crystal structures of the calcium pump and sarcolipin in the Mg2+-bound E1 state. Nature *495*, 260–264.

Tsai, F.C., Seki, A., Yang, H.W., Hayer, A., Carrasco, S., Malmersjö, S., and Meyer, T. (2014). A polarized Ca2+, diacylglycerol and STIM1 signalling system regulates directed cell migration. Nat. Cell Biol. *16*, 133–144.

Tupling, A.R., Bombardier, E., Gupta, S.C., Hussain, D., Vigna, C., Bloemberg, D., Quadrilatero, J., Trivieri, M.G., Babu, G.J., Backx, P.H., et al. (2011). Enhanced Ca2+ transport and muscle relaxation in skeletal muscle from sarcolipin-null mice. Am. J. Physiol. Cell Physiol. *301*, C841–C849.

van Rooij, E., Quiat, D., Johnson, B.A., Sutherland, L.B., Qi, X., Richardson, J.A., Kelm, R.J., Jr., and Olson, E.N. (2009). A family of microRNAs encoded by myosin genes governs myosin expression and muscle performance. Dev. Cell *17*, 662–673.

Vangheluwe, P., Schuermans, M., Zádor, E., Waelkens, E., Raeymaekers, L., and Wuytack, F. (2005). Sarcolipin and phospholamban mRNA and protein expression in cardiac and skeletal muscle of different species. Biochem. J. *389*, 151–159.

Wawrzynow, A., Theibert, J.L., Murphy, C., Jona, I., Martonosi, A., and Collins, J.H. (1992). Sarcolipin, the "proteolipid" of skeletal muscle sarcoplasmic reticulum, is a unique, amphipathic, 31-residue peptide. Arch. Biochem. Biophys. *298*, 620–623.

Wegener, A.D., Simmerman, H.K., Lindemann, J.P., and Jones, L.R. (1989). Phospholamban phosphorylation in intact ventricles. Phosphorylation of serine 16 and threonine 17 in response to beta-adrenergic stimulation. J. Biol. Chem. *264*, 11468–11474.

Winther, A.M., Bublitz, M., Karlsen, J.L., Møller, J.V., Hansen, J.B., Nissen, P., and Buch-Pedersen, M.J. (2013). The sarcolipin-bound calcium pump stabilizes calcium sites exposed to the cytoplasm. Nature *495*, 265–269.

Zhang, Y. (2008). I-TASSER server for protein 3D structure prediction. BMC Bioinformatics *9*, 40.

Cell

EXTENDED EXPERIMENTAL PROCEDURES

Radioisotopic In Situ Hybridization

Mouse embryonic and fetal sections were deparaffinized, permeabilized, and acetylated before hybridization at 55°C with riboprobes diluted in a hybridization solution (50% formamide, 0.3 M NaCl, 20 mM Tris-HCl [pH 8.0], 5 mM EDTA [pH 8.0], 10 mM $NaPO_4$ [pH 8.0], 10% dextran sulfate, 1x Denhardt's solution and 0.5 mg ml^{-1} tRNA). After hybridization, the sections were washed with increasing stringency, subjected to RNase A treatment (2 μg ml^{-1}, 30 min at 37°C) and dehydrated before dipping in K.5 nuclear emulsion gel (Ilford). Autoradiographic exposure ranged from 21 to 28 days. ^{35}S-labeled antisense probes were in vitro transcribed by Sp6 or T7 RNA polymerases using linearized cDNA templates using a Maxiscript kit (Ambion). The primer sequences used to clone MLN, PLN and SLN cDNA templates are listed in Table S2.

Treadmill Running

Mice were trained for 5 min at 7 m min^{-1} for 2 consecutive days prior to the running experiment. Following training, mice were run at 8 m min^{-1} for 30 min, followed by 9 m min^{-1} for 15 min and then 10 m/min for 15 min. The speed was increased 1 m min^{-1} every 10 min until exhaustion was reached. Exhaustion was indicated by refusal to run in response to electrical stimuli for greater than 5 s.

Intracellular Ca^{2+} Imaging

Retroviral transduced C2C12 cells or primary myoblasts were plated on Ibidi μ-35 mm tissue-culture dishes and cultured for 24 hr in low Ca^{2+} (0.1 mM Ca^{2+}) prior to imaging to increase sensitivity to changes in SR Ca^{2+} levels (Brandman et al., 2007). Cells were loaded with 0.5 μM fura-2-AM in extracellular buffer (ECB) containing 0.05% Pluronic F-127 and 0.1% of BSA for 30 min at room temperature and washed twice with ECB before imaging. Release of SR Ca^{2+} was induced by the addition of 1 mM 4-CMC (final concentration) in ECB in the presence of 3 mM EGTA. Changes of intracellular Ca^{2+} levels were indicated by the change of ratio of fluorescence intensity at 510 nm excited at 340 nm to that at 380 nm (F340/F380). SR Ca^{2+} levels were directly measured using T1ER (Abell et al., 2011; Tsai et al., 2014). T1ER retroviral transduced C2C12 cells were plated on Ibidi μ-35 mm tissue-culture dishes and cultured for 24 hr in 0.1 mM Ca^{2+} prior to imaging. CFP, FRET (CFP excitation and YFP emission), and YFP images of T1ER expressed cells were collected at 20X magnification. YFP images were used to define the regions of interest. The FRET intensity of each region was background-subtracted and normalized to the CFP image. Statistical analyses were performed using an unpaired t test and data are presented as mean ± SEM. Statistical significance is indicated with an "*" for p values less than 0.05. Experiments were performed in triplicate and repeated at least twice. Data are shown from a single representative experiment.

Oxalate-Supported Ca^{2+} Uptake Measurements in HEK293 Lysates

HEK293 cells were co-transfected with equal amounts of an expression plasmid encoding mouse SERCA1 and an expression plasmid encoding MLN, PLN or SLN. Approximately 36 hr after transfection, HEK293 cells were homogenized in 50 mM phosphate buffer (pH 7.0) containing 10 mM NaF, 1 mM EDTA, 0.3 M sucrose, 0.3 mM PMSF and 0.5 mM DTT. Ca^{2+} uptake was measured in reaction solution containing 40 mM imidazol (pH 7.0), 95 mM KCl, 5 mM NaN_3, 5 mM $MgCl_2$, 0.5 mM EGTA, 5 mM K^+ oxalate, 1 uM ruthenium red and various concentrations of $CaCl_2$ to yield 0.02 to 5 μM free Ca^{2+}. Homogenates were incubated at 37°C for 2 min in the above reaction buffer and the reaction was initiated by the addition of ATP (final concentration 5 mM). The data were analyzed by nonlinear regression with computer software (GraphPad Software), and the K_{Ca} values were calculated using an equation for a general cooperative model for substrate activation. The values for maximal SERCA activity were taken directly from the experimental data and normalized for total protein concentration (nmol Ca^{2+}/mg protein/min). Statistical analyses were performed using an unpaired t test and data are presented as mean ± SEM. Experiments were performed in triplicate and repeated at least twice. Data are shown from a single representative experiment.

Coimmunoprecipitations and Western Blot Analysis

Myc- and HA-epitope fusion proteins were co-expressed in COS7 cells and whole cell lysates were prepared in CoIP buffer (20 mM $NaPO_4$, 150 mM NaCl, 2 mM $MgCl_2$, 0.1% NP-40, 10% Glycerol, 10 mM sodium fluoride, 0.1 mM sodium orthovanadate, 10 mM sodium pyrophosphate, 1 mM DTT and Complete protease inhibitor [Roche]). Immunoprecipitations were carried out using 1 μg of mouse monoclonal anti-Myc antibody (Invitrogen) and captured on Protein A/G agarose beads (Santa Cruz Biotechnology). Western blots were performed as previously described using anti-HA (1:1,000, Invitrogen) and anti-Myc (1:5,000, Invitrogen) antibodies. Tris-tricine-SDS PAGE was carried out using 16.5% tris-tricine gels (BioRad) and tris-tricine-SDS running buffer (BioRad).

Electrophoretic Mobility Shift Assays

Recombinant Myc-tagged proteins used in electrophoretic mobility shift assays (EMSAs) were expressed in COS7 cells using transient transfection with Fugene6 and protein lysates were prepared in a similar manner as for CoIPs. Double-stranded EMSA probes were created by annealing complementary oligonucleotides in sodium chloride-Tris-EDTA buffer (50 mM NaCl, 10 mM Tris [pH 8.0], and 1 mM EDTA). Probe sequences are listed in Table S2. Binding reactions were carried out at room temperature in binding buffer (15% glycerol, 100 mM KCL, 10 mM Tris [pH 7.4], 1 mM DTT) and separated using PAGE. Supershifts were performed by adding 1 μg of mouse anti-Myc antibody (Invitrogen).

Luciferase Assays

COS7 cells were seeded at 4 × 10^4 cells per well in DMEM supplemented with 10% Fetal Bovine Serum in 24-well tissue-culture plates. Each well was transfected with a total of 400 ng of plasmid DNA using Fugene6 (Promega) 24 hr after seeding. Briefly, cells in each well were lysed in 200 μl of Passive Lysis Buffer (Promega) 24 hr after transfection and subjected to a single freeze–thaw cycle at −80°C. Luciferase activity was measured for each well by reacting 20 μl of cell lysate with 50 μl of Luciferase Assay Buffer (Promega) in white 96-well plates, using a FluoStar OPTIMA microplate reader (BMG Labtech). Individual wells were normalized to Beta-Galactosidase activity using the FluoReporter LacZ/Galactosidase Quantitation Kit (Invitrogen).

Subcellular Fractionation

C2C12 myoblasts were infected with a retrovirus encoding the HA-MLN fusion protein (pBabeX-HA-MLN). After 24 hr of infection, cells were dounce homogenized in hypotonic buffer (10 mM Tris [pH8.0], 1 mM EDTA plus Complete protease inhibitor [Roche]) and spun at 1,000 × *g* for 5 min to pellet cell debris. The homogenate was then spun at 12,000xg for 10 min to pellet SR/ER membrane proteins and heavy vesicles (P12 g fraction). The homogenate was spun at 100,000xg for 20 min using an ultracentrifuge to pellet plasma membrane proteins (P100 g fraction). The remaining homogenate was kept as the cytosolic fraction. For SDS-PAGE gel electrophoresis, the P12 g and P100 g pellets were solubilized in lysis buffer (50 mM Tris, [pH7.4], 150 mM NaCl, 1 mM EDTA, 1% Triton X-100, and Complete protease inhibitor [Roche]). Enrichment for each subcellular fraction was confirmed by western blot analysis using antibodies for each of the following proteins: Cytosolic - Hsp90 (F-8, Santa Cruz); SR/ER membrane - PDI (Cell Signaling) and plasma membrane - N-Cadherin (Cell Signaling).

Circular Dichroism Spectroscopy

Circular dichroism (CD) spectroscopy measurements were done using a JASCO J-815 spectrometer. Full-length MLN (Peptide 2.0) was diluted to 0.1 mg ml^{-1} in 50 mM sodium phosphate buffer (pH 7.4) and 0.1% n-Dodecyl-β-D-maltoside (DDM). The far-UV spectra of the peptide solution was measured at 20°C from 195 to 250 nm with the following instrument settings [response: 1 s, sensitivity: 20 mdeg, speed: 50 nm min^{-1}, path length: 1 mm] for an average of 20 scans. The secondary structure elements were calculated using Yang's fit. The RMS deviation for the observed and calculated CD spectra values was 3%.

Adult Muscle Electroporation and Imaging

Flexor digitorum brevis (FDB) muscles of 12-week old male mice were electroporated as previously described (Nelson et al., 2013). Three days following electroporation, unfixed FDB muscles were examined directly using two-photon laser scanning microscopy (Zeiss; LSM 780) with reverse second harmonic generation to visualize the A bands as an internal reference. MLN, PLN and SLN expression vectors were cloned into the CS2 vector containing an N-terminal green fluorescent (GFP) (see Table S2 for cloning details). Additionally, the coding sequence of mouse SERCA1 was cloned into the CS2 vector containing an N-terminal mCherry fluorescent protein (mCherry-SERCA1) and co-electroporated with GFP-MLN (see Table S2 for cloning details). All constructs were sequenced verified.

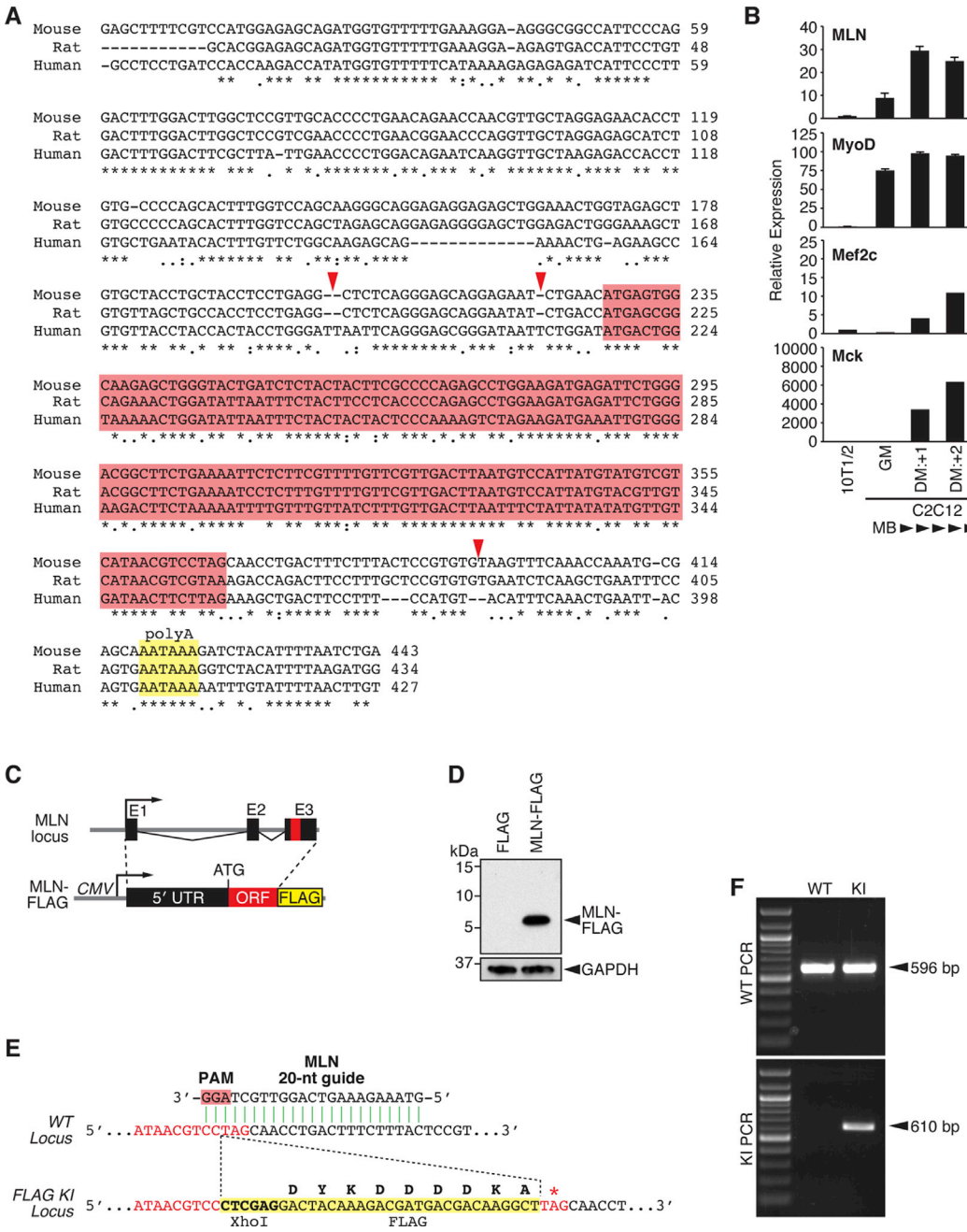

Figure S1. Conservation and Expression of the MLN Transcript and Micropeptide, Related to Figure 1

(A) Multiple sequence alignment of human, mouse, and rat MLN transcripts. The conserved polyadenylation (polyA) sequence is highlighted in yellow. The MLN coding sequence is highlighted in maroon and the flanking sequence insertions and deletions that restrict the coding potential of MLN are indicated (red arrows).

(B) Relative expression of MLN in mouse 10T1/2 fibroblasts and mouse C2C12 myoblasts (MB) cultured in growth medium (GM) or differentiated into myotubes (MT) in differentiation medium (DM). MLN is expressed in both myoblasts and myotubes, similar to the expression of MyoD, but different from Mef2c and MCK, which are specifically upregulated upon myoblast differentiation. Data are presented as mean ± SEM.

(C) Diagram showing the location of the FLAG epitope tag inserted in-frame with the C terminus of the MLN coding sequence within the MLN transcript (MLN-FLAG).

(D) Western blot analysis showing expression of the MLN-FLAG fusion peptide in COS7 cells detected with an anti-FLAG antibody.

(E) Genomic sequence of the mouse MLN endogenous locus targeted by CRISPR/Cas9 to knockin a FLAG epitope tag. The FLAG knockin locus contains a C-terminal FLAG tag in-frame with the MLN coding sequence.

(F) PCR-based genotyping results for the WT and MLN-FLAG knockin (KI) allele.

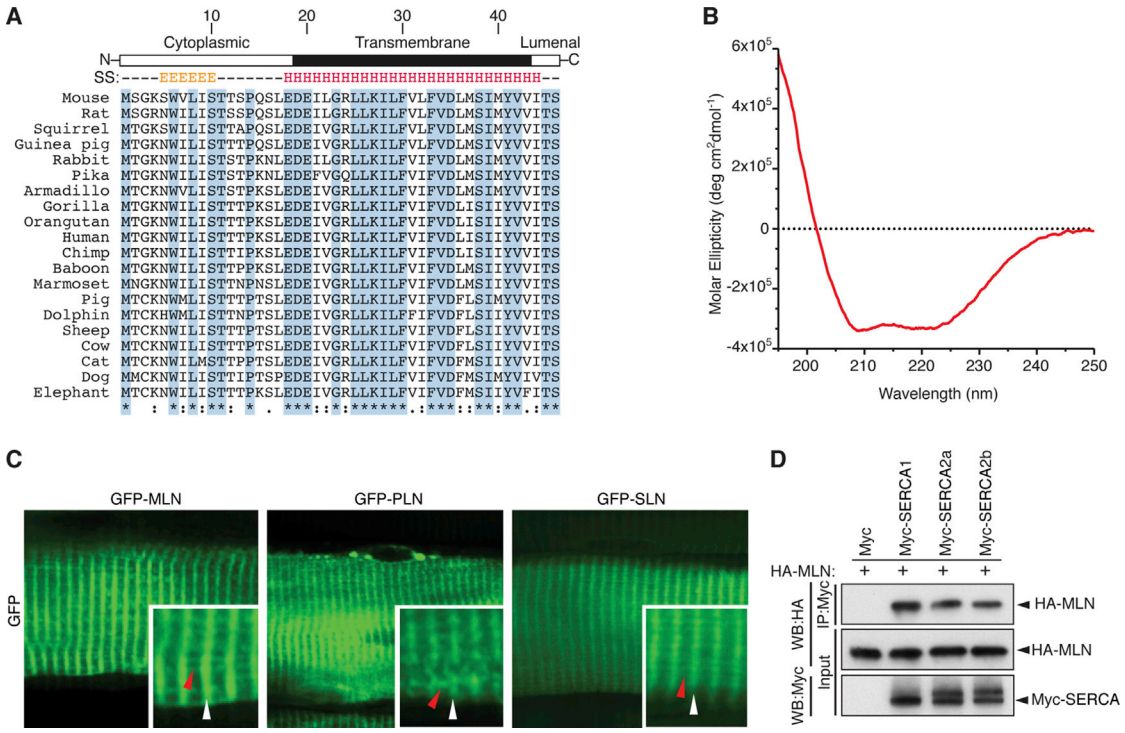

Figure S2. MLN Encodes a Transmembrane Alpha Helix and Interacts with SERCA in the SR, Related to Figure 2

(A) The secondary structure (SS) of MLN is predicted to contain an N-terminal beta sheet and C-terminal transmembrane alpha helix (E, beta sheet; H, alpha helix). Sequence alignment of the MLN micropeptide shows high conservation across multiple species.

(B) Circular dichroism spectroscopy measurements of a synthesized full-length MLN peptide in detergent micelles confirmed it consists of both alpha helix and beta sheet secondary structures.

(C) Electroporation and transient expression of a GFP-MLN fusion protein in mature skeletal muscle fibers showed localization in the longitudinal (red arrow) and junctional (white arrow) regions of the SR, similar to the pattern observed for GFP-PLN and GFP-SLN fusion proteins.

(D) Co-immunoprecipitation experiments were performed from transfected COS7 cells using an HA-MLN fusion peptide and Myc-tagged SERCA isoforms (Myc-SERCA1, Myc-SERCA2a, and MT-SERCA2b). Western blot analysis revealed that HA-MLN formed a stable complex with different isoforms of SERCA, similar to previous reports of the PLN- and SLN-SERCA interactions.

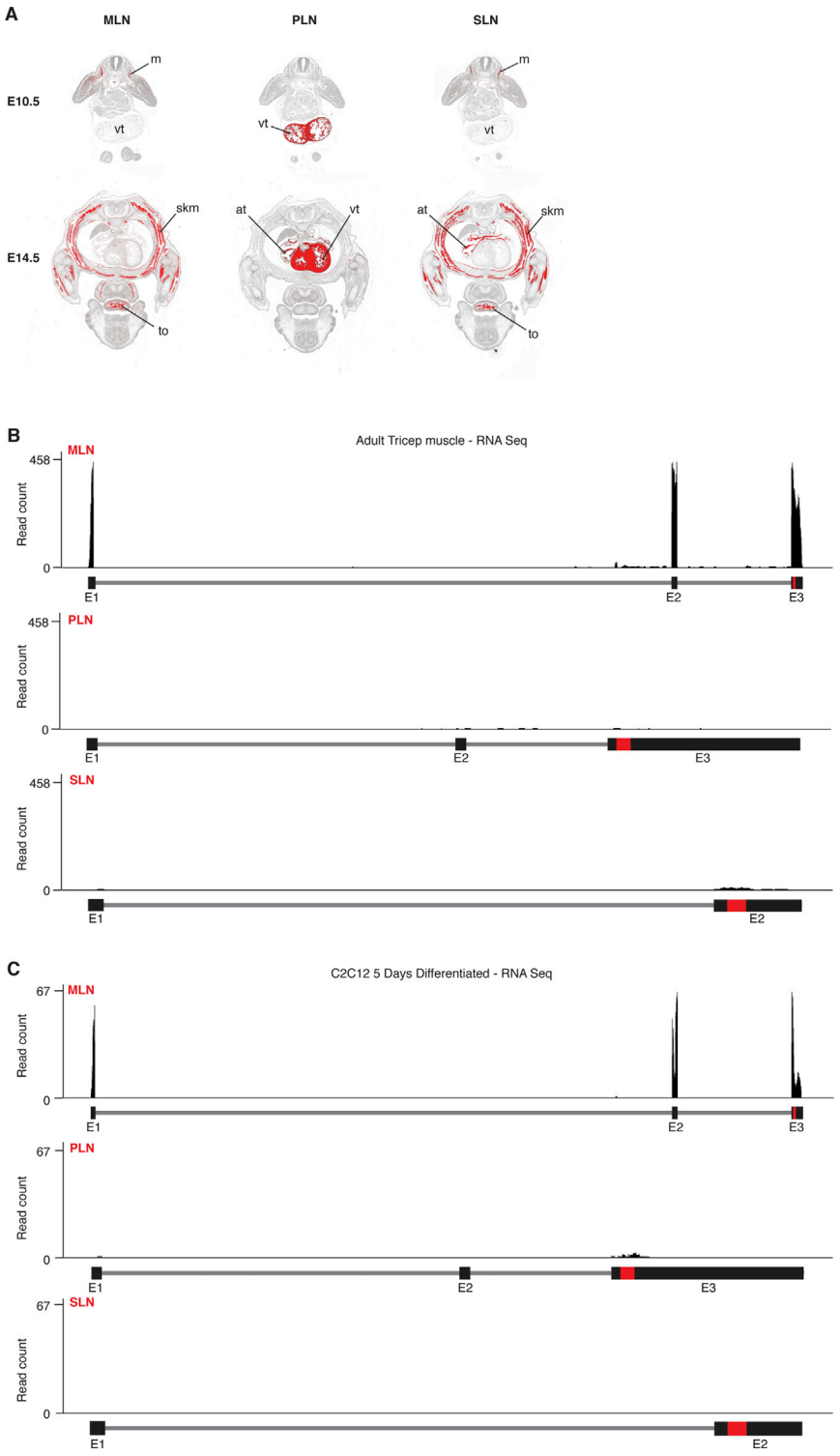

Figure S3. Expression of MLN, PLN, and SLN in the Mouse, Related to Figure 4

(A) In situ hybridization using probes specific for MLN, SLN or PLN during mouse developmental stages E10.5 and E14.5. (at, atria; m, myotome; skm, skeletal muscle; to, tongue; vt, ventricle)

(B and C) RNA-seq data corresponding to MLN, PLN and SLN transcripts in adult triceps muscle and C2C12 myotubes differentiated for 5 days showed that MLN is abundant in these tissues while PLN and SLN are expressed at background levels.

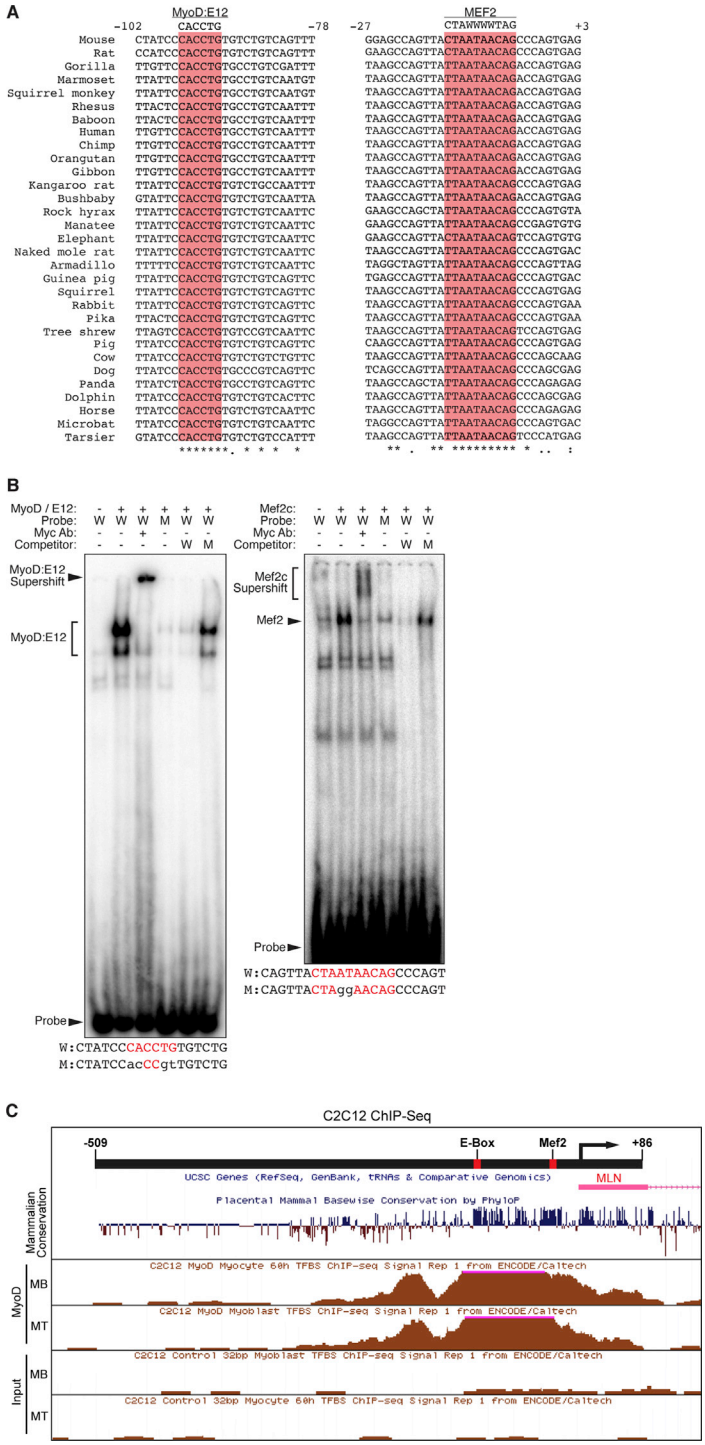

Figure S4. Regulation of MLN Transcription by MyoD and MEF2, Related to Figure 5

(A) Sequence alignment of the conserved MyoD E-box and Mef2 sites in the MLN promoter. The position weight matrix score for both sites was calculated for the mouse sequence using MATCH (E-box: V$MYOD_Q6, core = 1.00 and PWM = 0.932) (Mef2: V$MEF2_02, core = 0.853 and PWM = 0.717).

(B) Electromobility shift assays (EMSAs) demonstrate that these sites were specifically bound by MyoD:E12 heterodimer and Mef2c. W, wild type; M, mutant.

(C) ChIP-seq data available for C2C12 myoblasts or myotubes showed that the region containing the E-box and MEF2 sites is strongly bound by MyoD. Input track data are shown as a control.

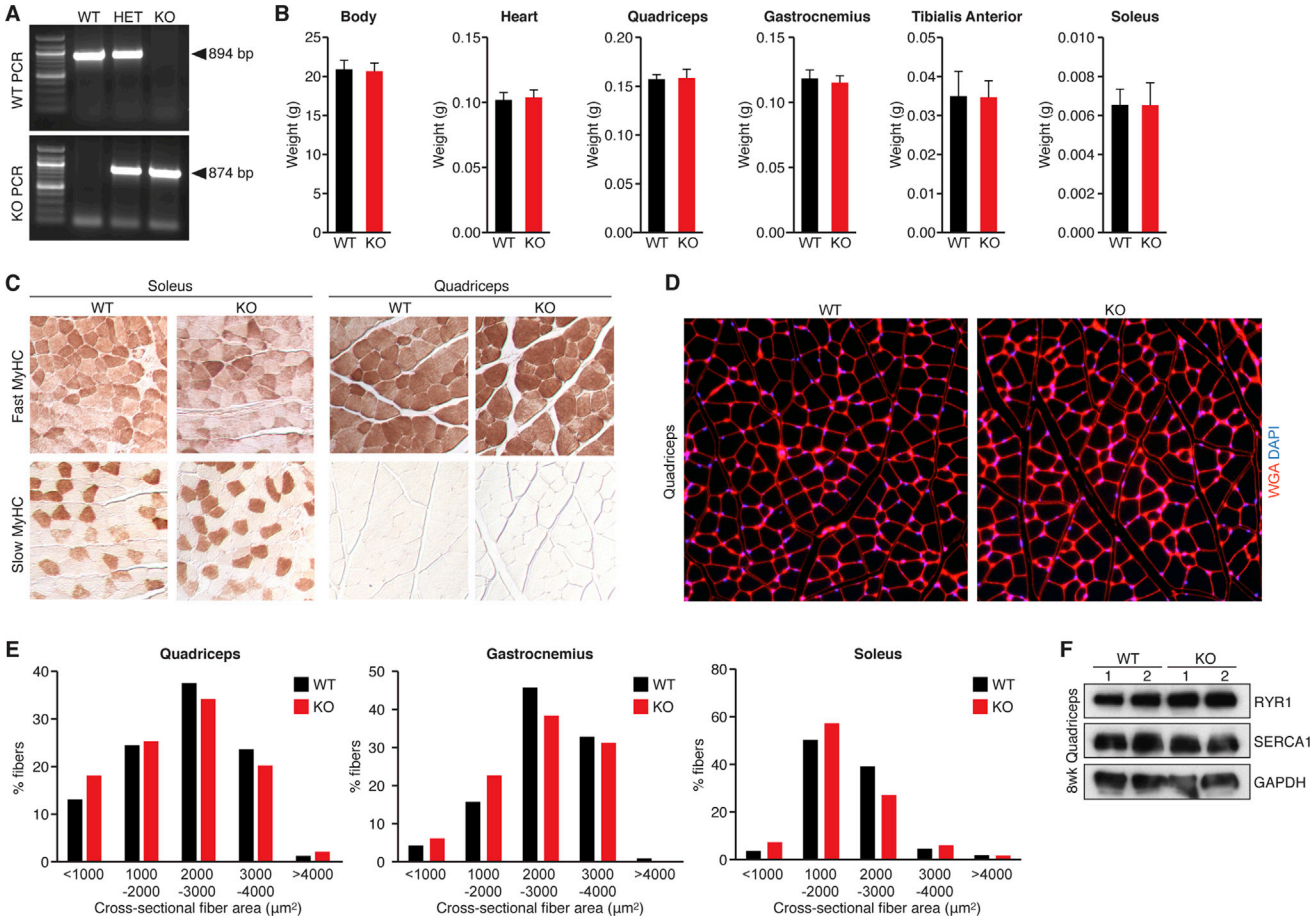

Figure S5. MLN KO Confirmation and Histological Analysis, Related to Figure 6

(A) PCR genotyping using primers outside of the donor homology arms confirmed the genotype of WT, MLN-heterozygous and -KO mice

(B) Body, heart and muscle weights were similar for WT and MLN KO mice. Data are presented as mean ± SEM.

(C) Immunohistochemistry for fast and slow type myofibers in soleus and quadriceps muscles of WT and MLN KO mice were similar.

(D and E) Wheat germ agglutinin (WGA) staining was used to define myofiber area in quadriceps, gastrocnemius, and soleus muscles. No obvious differences in myofiber area were found in MLN-KO muscle compared to WT littermates.

(F) Western blot analysis showing similar levels of expression of RyR1 and SERCA1 expression in quadriceps muscles isolated from two separate WT and MLN KO animals.